

Supporting Information:

Headgroup structure and cation binding in

phosphatidylserine lipid bilayers

Hanne Antila,[†] Pavel Buslaev,[‡] Fernando Favela,[¶] Tiago M. Ferreira,[§] Ivan Gushchin,[‡] Matti Javanainen,^{||} Batuhan Kav,[†] Jesper J. Madsen,[⊥] Josef Melcr,[#] Markus Miettinen,[†] Ricky Nencini,[#] O. H. Samuli Ollila,^{*,#} and Thomas Piggot[△]

[†]*Department of Theory and Bio-Systems, Max Planck Institute of Colloids and Interfaces,
14424 Potsdam, Germany*

[‡]*Moscow Institute of Physics and Technology*

[¶]*Mexico*

[§]*Halle, Germany*

^{||}*Institute of Organic Chemistry and Biochemistry of the Czech Academy of Sciences,
Flemingovo nám. 542/2, CZ-16610 Prague 6, Czech Republic*

[⊥]*Department of Chemistry, The University of Chicago, Chicago, Illinois 60637, United
States of America*

[#]*Institute of Organic Chemistry and Biochemistry, Academy of Sciences of the Czech
Republic, Prague 6, Czech Republic*

[@]*Institute of Biotechnology, University of Helsinki*

[△]*Southampton, United Kingdom*

E-mail: samuli.ollila@helsinki.fi

S1 Simulated systems

S1.1 CHARMM36

POPC bilayer. Previously published values²⁴ calculated from the data available from Ref. 25 are used.

DOPS and POPS bilayers.

The data in Table I and Refs 26–28 T. Piggot, please write simulation details

POPC:POPS mixtures without additional ions

Simulations of POPC:POPS (5:1) mixture containing total 132 (110:22) lipids with potassium and sodium counterions were ran using CHARMM36 force field. The data are available from Refs. 5 and 8, respectively T. Piggot, please write simulation details.

Simulations of POPC:POPS (5:1) and POPC:POPS (1:1) mixtures containing total 300 lipids with potassium counterions were ran using CHARMM36 force field. The data are available from Refs. 4 and 29 J. Madsen, please write simulation details.

POPC:POPS (5:1) mixtures with additional monovalent ions. POPC:POPS (110:22) mixtures containing total 132 lipids with the additional potassium or sodium ions corresponding concentrations of ~450 mM and 890 mM were generated with the CHARMM-GUI.^{30,31} Systems were simulated using Gromacs 5³² and CHARMM36 force field with the simulation parameters given by the CHARMM-GUI at 298 K. For further details, simulation files and data, see table S1 and Refs. 6,7,9,10.

POPC:POPS (5:1) mixtures with additional calcium

POPC:POPS (5:1) mixtures containing total 300 (250:50) lipids were simulated with the additional calcium concentrations. The data is available from Refs. 33 and 34. J. Madsen, please write simulation details.

Table S1: The list of POPC:POPS mixtures simulated with different amounts of added monovalent ions. The salt concentrations are calculated as $[\text{salt}] = N_c \times [\text{water}] / N_w$, where $[\text{water}] = 55.5 \text{ M}$. This corresponds the concentration in buffer before solvating lipids, which are reported in the experiments by Roux et al.¹

lipid/counter-ions	force field for lipids / ions	^a C _{ci} (M)	^b N _i	^c N _w	^d N _c	^e T (K)	^f t _{sim} (ns)	^g t _{anal} (ns)	^h files
POPC:POPS (5:1)/K ⁺	CHARMM36 ^{2,3}	0	250:50	11207	0	298	200	180	4
POPC:POPS (5:1)/K ⁺	CHARMM36 ^{2,3}	0	110:22	4620	0	298	500	100	5
POPC:POPS (5:1)/K ⁺	CHARMM36 ^{2,3}	0.45	110:22	4926	40	298	200	150	6
POPC:POPS (5:1)/K ⁺	CHARMM36 ^{2,3}	0.89	110:22	4946	79	298	200	150	7
POPC:POPS (5:1)/Na ⁺	CHARMM36 ^{2,3}	0	110:22	4620	0	298	500	100	8
POPC:POPS (5:1)/Na ⁺	CHARMM36 ^{2,3}	0.44	110:22	4965	39	298	200	150	9
POPC:POPS (5:1)/Na ⁺	CHARMM36 ^{2,3}	0.89	110:22	4932	79	298	200	150	10
POPC:POPS (5:1)/K ⁺	MacRog ¹¹	0	120:24	5760	0	298	400	250	12
POPC:POPS (5:1)/K ⁺	MacRog ¹¹	0.50	120:24	5760	52	298	300	200	13
POPC:POPS (5:1)/K ⁺	MacRog ¹¹	1.00	120:24	5760	104	298	300	200	13
POPC:POPS (5:1)/K ⁺	MacRog ¹¹	2.00	120:24	5760	208	298	300	200	13
POPC:POPS (5:1)/K ⁺	MacRog ¹¹	3.00	120:24	5760	311	298	300	200	13
POPC:POPS (5:1)/K ⁺	Lipid14/17 ^{14,15}	0	120:24	5760	0	298	500	200	16
POPC:POPS (5:1)/K ⁺	Lipid14/17 ^{14,15}	0.50	120:24	5760	54	298	300	200	17
POPC:POPS (5:1)/K ⁺	Lipid14/17 ^{14,15}	1.00	120:24	5760	104	298	300	200	17
POPC:POPS (5:1)/K ⁺	Lipid14/17 ^{14,15}	2.00	120:24	5760	208	298	300	200	17
POPC:POPS (5:1)/K ⁺	Lipid14/17 ^{14,15}	3.00	120:24	5760	311	298	300	200	17
POPC:POPS (5:1)/K ⁺	Lipid14/17 ^{14,15}	4.00	120:24	5760	415	298	300	200	17
POPC:POPS (5:1)/Na ⁺	Lipid14/17 ^{14,15}	0	120:24	5760	0	298	500	200	18
POPC:POPS (5:1)/Na ⁺	Lipid14/17 ^{14,15}	0.50	120:24	5760	54	298	300	200	19
POPC:POPS (5:1)/Na ⁺	Lipid14/17 ^{14,15}	1.00	120:24	5760	104	298	300	200	19
POPC:POPS (5:1)/Na ⁺	Lipid14/17 ^{14,15}	2.00	120:24	5760	208	298	300	200	19
POPC:POPS (5:1)/Na ⁺	Lipid14/17 ^{14,15}	3.00	120:24	5760	311	298	300	200	19
POPC:POPS (5:1)/Na ⁺	Lipid14/17 ^{14,15}	4.00	120:24	5760	415	298	300	200	19
POPC:POPS (4:1)/Na ⁺	Berger ^{20,21}	0	102:26	4290	0	310	120	80	22
POPC:POPS (4:1)/Na ⁺	Berger ^{20,21}	1.03	102:26	4290	80	310	200	50	23

^aExcess Na⁺ or K⁺ concentration

^bNumber of lipid molecules with largest mole fraction

^cNumber of water molecules

^dNumber of additional cations

^eSimulation temperature

^fTotal simulation time

^gTime used for analysis

^hReference for simulation files

S1.2 CHARMM36ua

DOPS and POPS bilayers.

The data in Table I and Refs 35,36 T. Piggot, please write simulation details

S1.3 MacRog

POPC bilayers. The POPC bilayer consisting of a total of 128 lipids was constructed from single lipid structure taken from Ref. 37. The bilayer was hydrated by a total of 5120 water molecules, corresponding to 40 water molecules per lipid. The MacRog lipid parameters,³⁸ obtained from Ref. 37, were used, along with the TIP3P water model.³⁹ The simulation parameters were identical to those used for POPC/POPC mixtures with the MacRog force field, see below. The simulation was run for 200 ns using Gromacs 2016.3,³² out of which 150 ns were used for analyses. The simulation data and related files are available from Ref. 40.

POPS bilayers.

The data in Table I and Refs 41,42 T. Piggot and M. Javanainen, please write simulation details

Piggot: please write about system with Na⁺ counterions.

This membrane was further simulated after replacing Na⁺ counterions by K⁺ ones, which were described by the Åqvist parameters.⁴³ Other topologies were unchanged. The simulation parameters were the same as used for the POPC/POPS mixtures with the MacRog force field, see below. The simulation was run for 200 ns, out of which 150 ns was used in the analyses.

POPC:POPS (5:1) mixtures with additional potassium ions

The bilayers containing a total of 120 POPC and 24 POPS molecules distributed evenly

among the two leaflets were set up using CHARMM-GUI.^{30,31} The bilayers were solvated by 5760 water molecules, corresponding to 40 water molecules for lipid. Additionally, 24 potassium ions were added to neutralize the charge of the POPS head groups. These bilayers were simulated using Gromacs 2016.3³² in the presence of counterions only, as well as together with different concentrations of CaCl₂ or KCl. For the former, concentrations of 100 mM, 300 mM, 1 M, and 3 M were considered, which corresponded to the amounts of 10/20, 31/62, 104/208, and 311/622 of Ca²⁺/Cl⁻ ions. For membranes with KCl, concentrations of 500 mM, 1 M, 2 M, and 3 M were considered, corresponding to 52, 104, 208, or 311 pairs of K⁺ and Cl⁻ ions.

The lipids were described using the MacRog model.^{11,38,44} The POPC topologies were obtained from Ref. 37, whereas the POPS topology was adapted from OPPS topology in Ref. 44 by reversing the order of acyl chains. The initial structures from CHARMM-GUI were used because they have the naturally occurring L stereoisomer in the POPS head group, instead of the D stereoisomer present in Ref. 44. TIP3P model³⁹ was used for water, and the Åqvist parameters,⁴³ standard for the OPLS force field, were employed for the ions.

The simulation parameters were taken from Ref. 44. Periodic boundary conditions were employed in all dimensions. The list of neighbors was updated every step. The Lennard-Jones interactions were cut off at 1 nm, whereas the smooth particle mesh Ewald algorithm⁴⁵ was used for electrostatics. Dispersion correction⁴⁶ was applied to both energy and pressure. Temperature was kept constant at 298 K using the Nosé–Hoover thermostat.^{47,48} The lipids and the solvent were coupled separately, and a time constant of 0.4 ps was employed. Pressure was maintained semi-isotropically at 1 bar using the Parrinello–Rahman barostat with a time constant of 1 ps.⁴⁹ All non-water bonds were constrained with the LINCS algorithm,^{50,51} whereas the bonds in water molecules were constrained using SETTLE.⁵² The integration time step was set to 2 fs, and the simulations were performed either for 400 ns (only counterions), 300 ns (systems with KCl), or 600 ns (systems with CaCl₂). The last 250, 200, or 300 ns of the simulations were included in the analyses, respectively.

S1.4 Lipid17

DOPS and POPS bilayers.

The structure of the bilayers with 128 DOPS or 128 POPS lipids were obtained from CHARMM-GUI.^{30,31} Bilayers are solvated with 4480 water molecules resulting in 31.1 water molecules per lipid. For each system, 128 NaCl molecules are added to neutralize the system. In all simulations, TIP3P⁵³ was used as the solvent. SETTLE⁵² algorithm was employed to constrain the bonds in TIP3P water molecules. Simulations were ran using Amber18 simulation package⁵⁴ and lipid parameters were obtained from Amber Lipid17 force field.¹⁵ For the ions, one set of simulations were run with Joung-Cheatham ion parameters⁵⁵ and one set of simulations were run with ff99SB (Åqvist)⁴³ ion parameters. The data in Table I and Refs 56–59 contain the number of molecules in simulations, related simulation files and trajectories.

Each bilayer structure was first minimized for 2500 steps with steepest descent and an additional 2500 step with the conjugent gradient algorithms while restraining the solvent and ion molecules with a force constant 500 kcal mol⁻¹ Å⁻¹. An additional minimization step was used with the same parameters after removing the constraints on the solvent and ion molecules. During the minimization procedure, non-periodic boundary conditions were applied, no pressure scaling was used and none of the bonds were restrained. A three step heating procedure was applied: in the first heating step the system temperature is increased from 0.0 K to 100.0 K using Langevin thermostat with 5.0 ps⁻¹ collision frequency while restraining the lipid positions with harmonic springs of force constant 20.0 kcal mol⁻¹ Å⁻¹ at constant volume without periodic boundary conditions. In the second heating step, the system temperature was increased from 100.0 K to 200.0 K using Langevin thermostat with 5.0 ps⁻¹ collision frequency within 10000 steps while restraining the lipid positions with harmonic springs of force constant 10.0 kcal mol⁻¹ Å⁻¹ at constant volume. In the third heating step, the system temperature is increased from 200.0 K to 303.0 K within 10000

steps using Langevin thermostat with 5.0 ps^{-1} collision frequency while restraining the lipid positions with harmonic springs of force constant $10.0 \text{ kcal mol}^{-1} \text{ \AA}^{-1}$ at 1 bar constant pressure using Berendsen barostat with 3.0 ps relaxation time. From the second heating step onward, periodic boundary conditions in all dimensions were applied. The semi-isotropic pressure coupling along xy -plane was employed and the surface tension was set to 0.0 dyn explicitely. After the third heating step, each structure is equilibrated for 100 ns at 1 bar and 303 K constant pressure using Berendsen barostat and temperature using Langevin thermostat, respectively. For the equilibration step, semi-isotropic pressure coupling along xy -plane was employed and the surface tension was set to 0.0 dyn explicitely. For all heating and equilibration steps, the lengths of the hydrogen containing bonds were restrained using SHAKE algorithm and a time step of 2 fs was used. In all steps with periodic boundary conditions, the non-bonded interactions are calculated with particle mesh Ewald⁴⁵ using 1.0 nm cutoff.

For the production runs, the temperature and pressure were set to 303 K and 1 bar, using Langevin thermostat with 1.0 ps^{-1} collision frequency and Berendsen barostat with 1.0 ps relaxation time, respectively. Periodic boundary conditions were applied in all dimensions and the non-bonded interactions are calculated with particle mesh Ewald⁴⁵ using 1.0 nm cutoff. The lengths of the hydrogen containing bonds were constrained using SHAKE algorithm and a time step of 2 fs was used. Trajectories are saved in every 10 ps intervals. Two independent trajectories of 500 ns long was generated and the last 200 ns portions were used for the analysis.

POPC:POPS (5:1) mixtures with additional potassium and sodium ions

The initial structure of the bilayers with 120 POPC and 24 POPS lipids were obtained from CHARMM-GUI.^{30,31} Bilayers were solvated with 5760 TIP3P water molecules.⁵³ For the simulations of the lipids and ions, the Amber Lipid 17¹⁵ and ff99SB⁴³ force fields were used,

respectively. Simulations were ran using Amber18 simulation package⁵⁴ The simulation steps are the same as the the simulations of DOPS and POPS bilayers described above, with the only difference that the total simulation time was 300 ns, of which last 200 ns was used for the analysis. The number of ions in each specific system is given in Table S1. The trajectory files can be found in Refs 16–19.

POPC:POPS (5:1) mixtures with additional calcium

One set of simulations of POPC:POPS (5:1) mixtures with additional calcium ions has been performed using Amber18 simulation package.⁵⁴ Number of ions and water molecules for this set of simulations are shown in Table II. The simulation details, minimization, heating, and equilibration runs are the same as described above for the other POPC:POPS (5:1) simulations with Amber Lipid17 forcefield. For all simulations, ff99SB⁴³ ion parameters and Amber lipid 17 force field were used. For each ion concentration, 100 ns equilibration runs were followed by 300 ns production runs with two independent trajectories, of which last 200 ns were used for the analysis. The trajectory files can be found in Ref 60

J. Melcr, please write simulation details about Gromacs simulations with Dang ions.

S1.5 Slipids

POPS POPS⁶¹ to be written by Piggot

DOPS with 128 lipids. DOPS with 128 lipids⁶² to be written by Piggot

DOPS with 288 lipids. The starting structure with 288 DOPS lipids, 11232 water molecules and 288 Na ions was contructed with the MEMBRANE BUILDER website.⁶³ The Slipids^{64,65} forcefield was used for DOPS, the TIP3P³⁹ water model was used to solvate the system and ions are described by the parameters derived by Åqvist.⁴³ The system was simulated in NPT ensemble for 200 ns using the GROMACS 5.0.4 package,³² and the last 100 ns was used

for the analysis. Timestep of 2 fs was used with the leapfrog integrator. The Nosé–Hoover thermostat^{47,48} was used with reference temperature of 303 K and a relaxation time constant of 0.5 ps; lipids and water plus ions were coupled separately to the heat bath. Pressure was kept constant at 1.013 bar using a semi-isotropic Parrinello–Rahman barostat⁴⁹ with a time constant of 10.0 ps. Long-range electrostatic interactions were calculated using the PME method.^{45,66} A real space cut-off of 1.0 nm was employed with grid spacing of 0.12 nm in the reciprocal space. Lennard-Jones potentials were cut off at 1.4 nm, with a dispersion correction applied to both energy and pressure. All covalent bonds in lipids were constrained using the LINCS algorithm,⁵⁰ whereas water molecules were constrained using SETTLE.⁵² Twin-range cutoffs, 1.0 nm and 1.6 nm, were used for the neighbor lists with the long-range neighbor list updated every 10 steps.

S1.6 Berger

POPC bilayers. Previously published simulation⁶⁷ available from Ref. 68 was used for POPC at 310 K.

DOPS and POPS bilayers.

The data in Table I and Refs 69,70 T. Piggot, please write simulation details

POPC:POPS (4:1) mixtures with additional sodium and calcium ions. Previously published simulations with the additional amount of sodium⁷¹ available from Ref. 23 and with the additional amounts of calcium⁷² available from Refs. 73,74 were used. To generate the reference system with sodium counterions only, the additional ions were removed from the structure file in Ref. 23. This system was simulated 120 ns using Gromacs 5³² with parameter (mdp file) and force field files (top and itp) available from Ref. 22, the last 80 ns was used for the analysis.

S1.7 GROMOS-CKP and GROMOS-CKPM

CKPM refers to the version with Berger/Chiu NH₃ charges compatible with Berger (i.e. the NH₃ group having the same charges as in the N(CH₃)₃ group of the PC lipids; 'M' stands for Mukhopadhyay after the first published Berger-based PS simulation that used these charges²¹) and CKP refers to the version with more Gromos compatible version (i.e. the charges for the NH₃ group taken from the lysine side-chain). **T. Piggot, please write the description of force field.**

DOPS and POPS bilayers.

The data in Table I and Refs. 75–78 **T. Piggot, please write simulation details**

POPC:POPS (5:1) mixtures without additional ions

The data in Table II and Refs. 79,80 **T. Piggot, please write simulation details**

S2 Electrometer concept in PC lipid bilayers mixed with negatively charged lipids

The electrometer concept is based on the empirical observations that the order parameters of α and β carbons in PC lipid headgroup decrease (increase) proportionally to the bound positive (negative) charge^{81–84} (Fig. S1). Therefore, the headgroup order parameters can be used to measure the ion binding affinity to lipid bilayers containing PC lipids.^{1,81–83,85,86} Changes of the headgroup order parameters of negatively charged PS and PG lipids are also systematic, but less well characterized.^{1,85–87} Therefore, the ion binding affinity to negatively charged bilayers can be better characterized measuring the PC headgroup order parameters from mixed bilayers.^{1,85–88}

When using the PC headgroup order parameters to evaluate the ion binding affinity to a bilayer containing anionic lipids, it is important to note that the order parameters increase

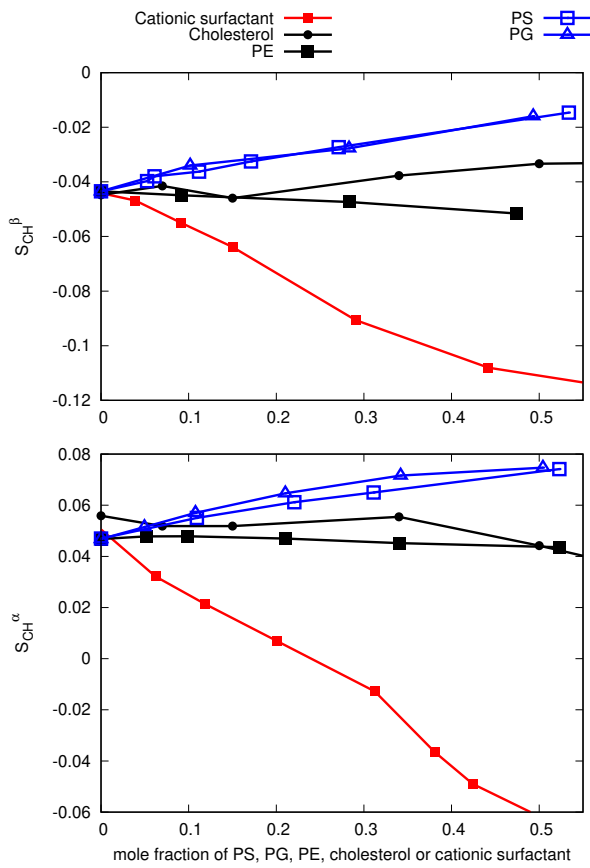


Figure S1: Headgroup order parameters of POPC measured from mixtures with PS (bovine brain), POPG, POPE, cholesterol and cationic dihexadecyldimethylammonium bromide (DHAB) surfactant.^{84,89,90} Signs are taken from separate experiments.^{91,92}

due to the addition of negative charged lipids according to the electrometer concept^{83,89} (Fig. S1). Therefore, the PC headgroup order parameters are larger in mixtures with anionic lipids than in pure lipid bilayers. This is evident also in the headgroup order parameters of POPC in bilayers with different amounts anionic lipids without added calcium (Fig. S2). Upon addition of CaCl_2 , the order parameters decrease and reach the values of pure PC bilayer close to the CaCl_2 concentrations of $\sim 50\text{-}300\text{mM}$, depending on the amount of negatively charged lipids in the mixture (Fig. S2). Around these concentrations the positive charge of bound Ca^{2+} cancels the negative charge lipids, resulting to a neutral membrane. Above such concentrations, the specific binding of calcium leads to the overcharging of the membrane.

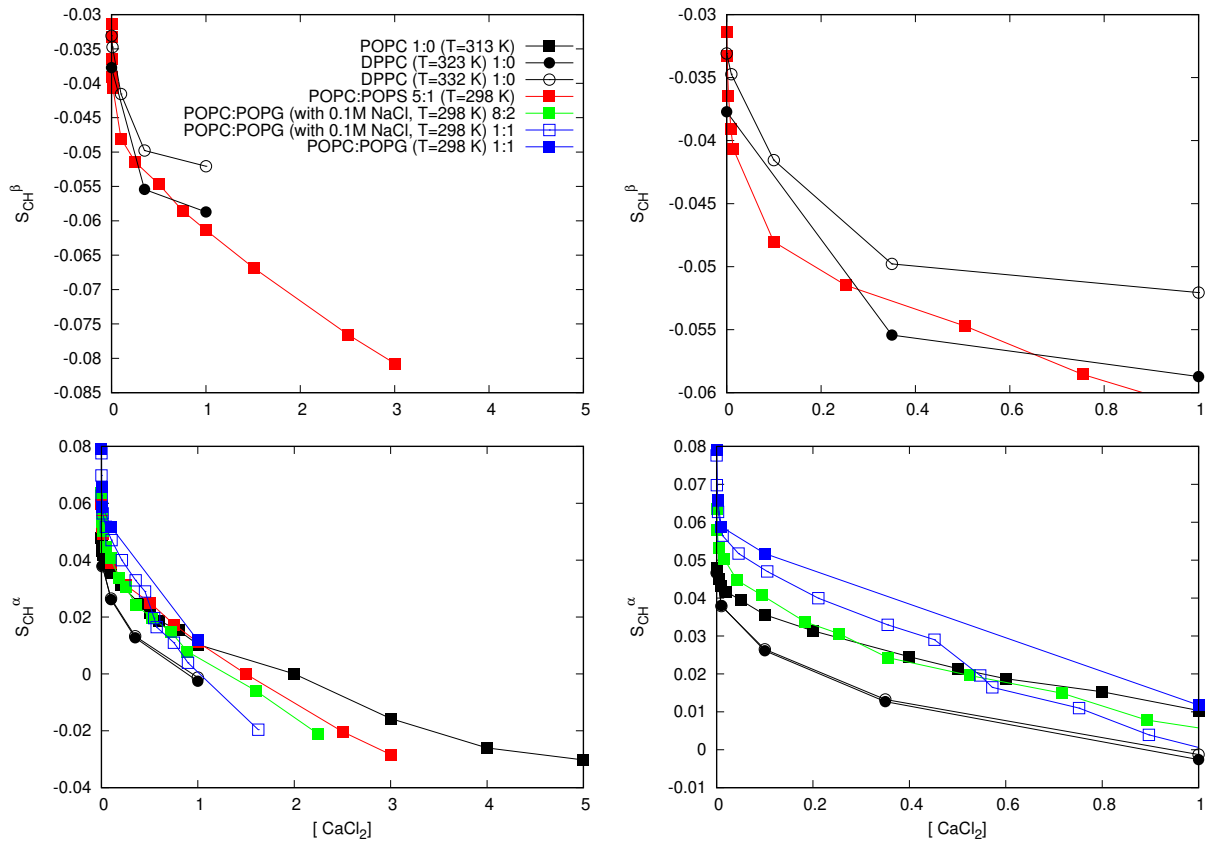


Figure S2: Headgroup order parameters of POPC as a function of CaCl_2 concentration from experiments with different mole fractions of negatively charged lipids (left column). Right column shows the same data zoomed to the concentrations below 1M. Data for Pure DPPC from Ref. 81, for pure POPC from Ref. 82, for POPC:POPS (5:1) mixture from Ref. 1, for POPC:POPG (8:2,1:1) mixtures with 0.1M NaCl from Ref. 86 and for POPC:POPG (1:1) mixture data without NaCl from Ref. 85.

Because the POPC headgroup order parameters in mixtures with different amounts of anionic lipids but without additional salt are not equal, the binding affinity of calcium can be better compared by plotting the changes of order parameters as a function of added calcium. As expected, such a plot reveals more pronounced order parameter decrease in systems with larger fractions of negatively charged lipids (Fig. S3), indicating an increase in the calcium binding affinity with the increasing amount of negatively charged lipids in membranes. In conclusion, the presented empirical comparison of headgroup order parameter changes from various mixtures of POPC and anionic lipids with added calcium gives physically consistent results, suggesting that the electrometer concept can be used to determine the cation binding affinity also to the lipid bilayers containing mixtures of PC and anionic lipids.

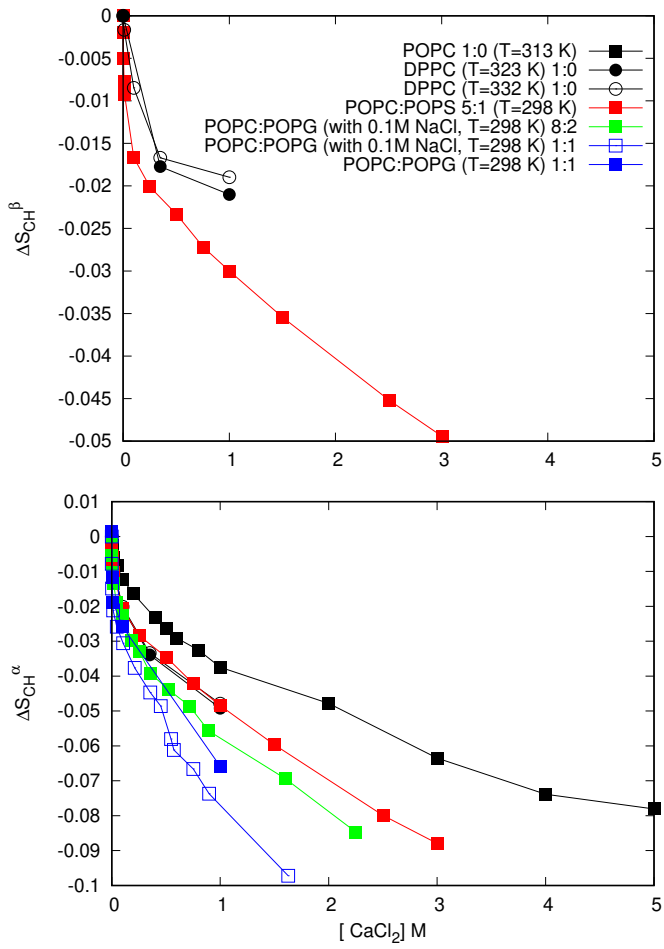


Figure S3: Changes of POPC headgroup order parameters as a function of CaCl_2 measured from mixed bilayers containing different amounts of anionic lipids. The original data is the same as in figure S2.

S3 Calibration of PC headgroup order parameter response to the bound cations

When using the molecular electrometer concept to compare ion binding affinity between simulations and experiments, one needs to keep in mind that two things affect how much a given order parameter changes when solution charge content is varied: 1) the change in the amount of bound charge and 2) the sensitivity of the order parameter to bound charge. Therefore, the response of the order parameters to the bound charge in simulations needs to be first calibrated against experiments.^{93,94}

In our previous work,⁹³ we investigated the change in order parameters under varying concentrations of mono- and divalent salts and concluded that the experimental $\Delta S_{\text{CH}}^{\beta}/\Delta S_{\text{CH}}^{\alpha}$ ratio⁸¹ was well reproduced by the Lipid14 model, but underestimated by other force fields. In a more recent study,⁹⁴ the headgroup order parameter responses were compared more carefully with the experiments of cationic dihexadecyldimethylammonium bromide (DHAB) surfactants in POPC bilayer.⁸⁴ The advantage of this approach is that the amount of DHAB in the bilayer is exactly known in experiments, which can be exploited to extract the sensitivity of the order parameters. This revealed that both S_{CH}^{β} and S_{CH}^{α} in the Lipid14 model are equally oversensitive (and thus giving the correct $\Delta S_{\text{CH}}^{\beta}/\Delta S_{\text{CH}}^{\alpha}$) to the bound charge, whereas CHARMM36 gives better agreement for the α carbon (Fig. S4), indicating that the headgroup order parameter response to the bound charge is actually more realistic in CHARMM36 compared to Lipid14. The ratio was overestimated for the CHARMM36 model because the β -carbon order parameter is relatively more sensitive than the α -carbon order parameter.

That said, in the force fields investigated so far, the discrepancies arising from the sensitivity of lipid headgroup to bound charge are typically smaller than the discrepancies arising from ion binding affinity.

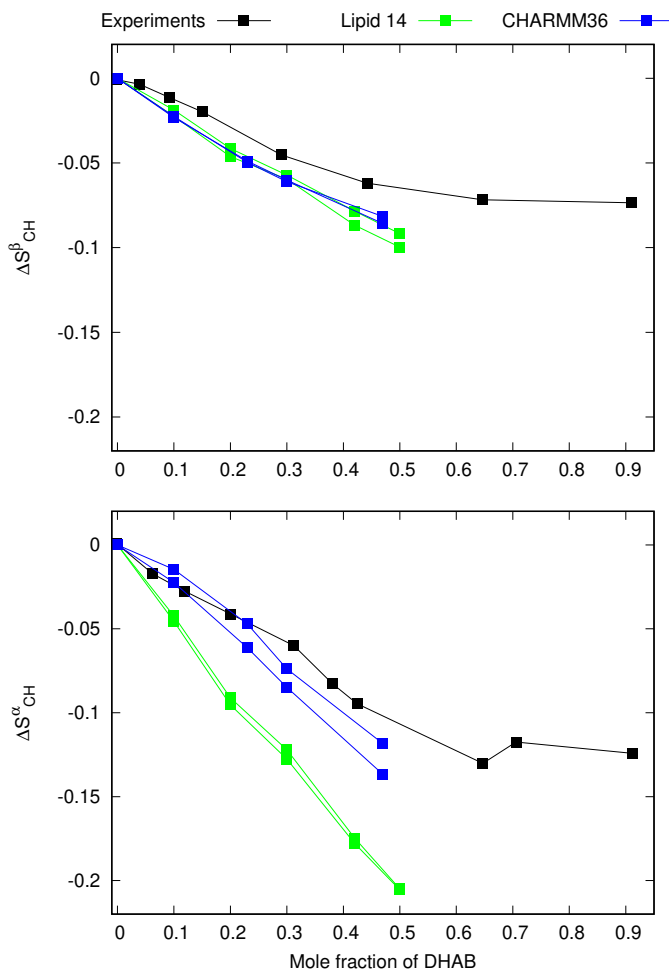


Figure S4: Responses of headgroup order parameters to the fixed amount of cationic surfactants in POPC bilayer from simulations and experiments.⁸⁴ The simulation results for Lipid14 are directly from Ref. 94. The CHARMM36 simulation data and details are available from Ref. 95.

S4 Sensitivity of the molecular electrometer to the chosen definition of ion concentration

Previous studies using the electrometer concept to assess the ion binding affinity to lipid bilayers report ion concentrations either in water before solvating the lipids (buffer concentration)^{1,81,93} or in bulk water after solvating the lipids (bulk concentration).^{82,94} In this work, we use the former definition to be consistent with the experimental reference data.¹ The difference between these two concentrations increases with the increasing ion binding affinity. However, Fig. S5 demonstrates that in a model with realistic ion binding affinity⁹⁴ the deviation between the two definitions is negligible.

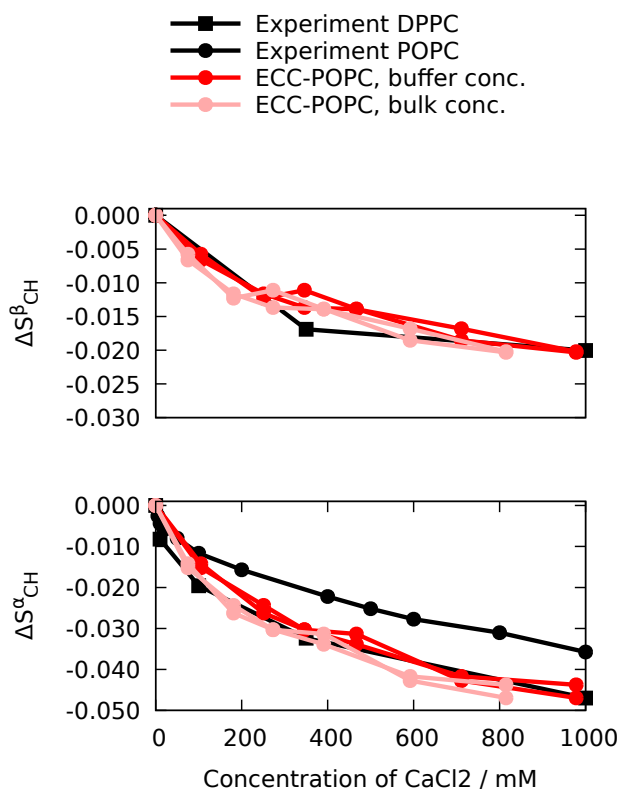


Figure S5: Changes of the headgroup order parameters as a function of CaCl_2 concentration using two possible definitions of ion concentration from the recent force field with realistic calcium binding affinity to a POPC bilayer⁹⁴ together with the experimental data.^{81,82}

S5 Spectral slices in the indirect dimension from the R-PDLF and SDROSS experiments

The C–H bond order parameters of the headgroup and glycerol backbone carbons are determined as $S_{\text{CH}} = \Delta\nu / (0.315 \times 21.5\text{kHz})$, where $\Delta\nu$ is the dipolar splitting given by the largest peak widths observed in the second dimension of the R-PDLF spectra (blue lines in Fig. S6), 0.315 is the scaling factor of the R18 recoupling sequence and 21.5 kHz is the maximum ^1H - ^{13}C dipolar coupling for a C–H bond.⁹⁶ The resulting order parameters are in good agreement with the previously reported values from ^2H NMR experiments⁹⁷ (Fig. 2 in the main text). However, the resolution in our ^{13}C NMR experiment was not sufficient to detect the the splitting related to the smaller order parameter of the C–H bond in the α carbon observed in ^2H NMR experiments.⁹⁷ Therefore, the value of 0 ± 0.02 from our ^{13}C NMR experiments is shown figure 2 and the magnitude of 0.02 from the literature is used in the SIMPSON calculations in the main text.

Interpretation of the order parameter signs of the α carbon from the SDROSS experiment is complicated by the presence of distinct order parameters for the two attached hydrogens. As discussed in the main text, interpretation of the SDROSS curve with the help of SIMPSON simulations gave values +0.09 and -0.02 for the α -carbon order parameters. To corroborate our interpretation, we measured the SDROSS curve also using the higher 8 kHz MAS frequence (Fig. S6 bottom), which makes the experiment more sensitive to larger order parameter values. Also this experiment indicates a positive value for the larger α -carbon order parameter.

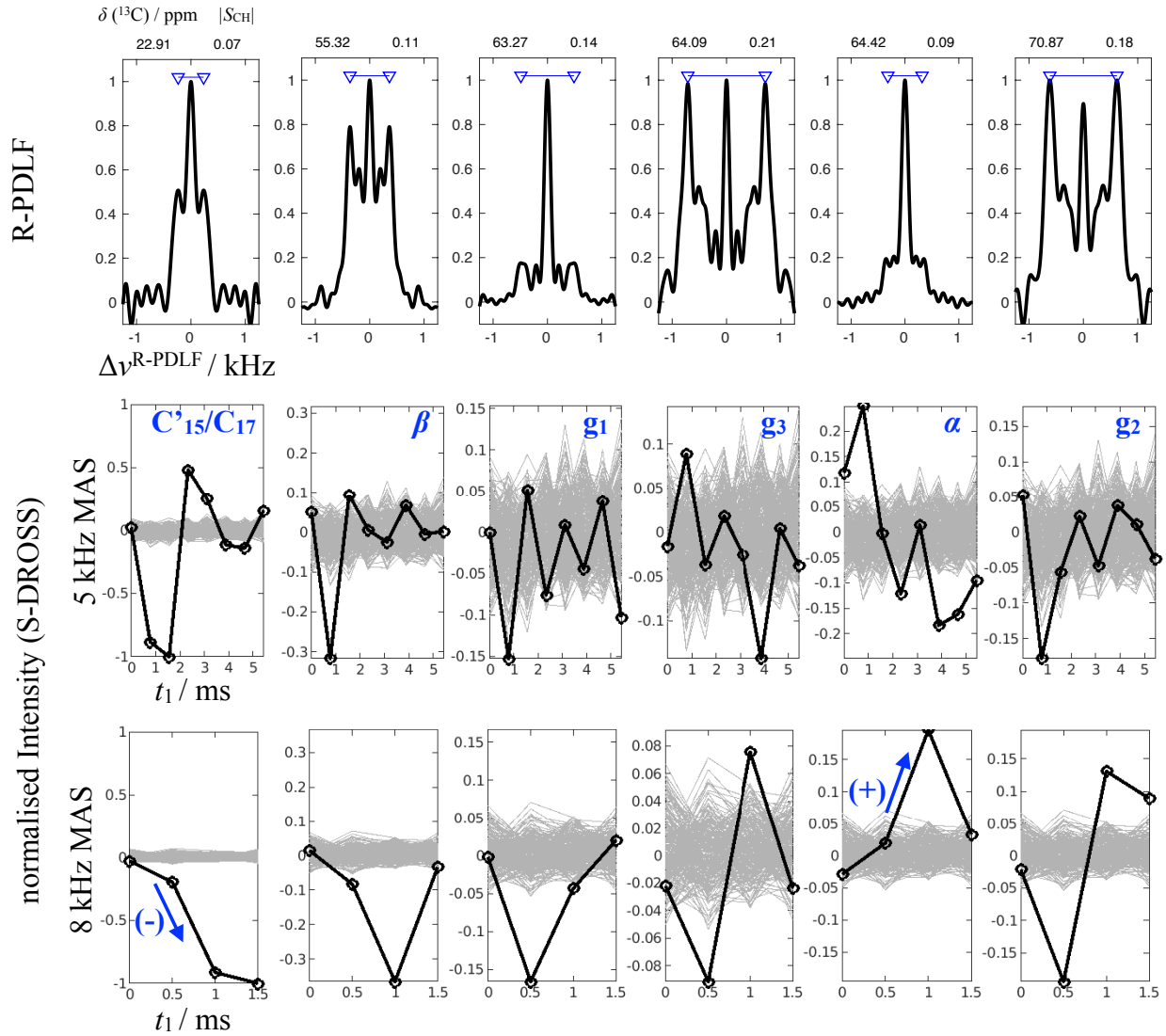


Figure S6: Spectral slices in indirect dimension from the R-PDLF (top) and S-DROSS (middle and bottom) experiments at distinct chemical shifts. The chemical shifts and order parameters (calculated from the dipolar splittings indicated with blue lines in the R-PDLF slices) are shown on top each column (chemical shift left, order parameter right). The assignment of columns is given in the middle. The SDROSS slices were measured using both 5 KHz (middle) and 8 kHz (bottom) because different MAS frequencies enable the higher sensitivity to the order parameters with lower and higher magnitudes, respectively. The background noise taken from chemical shift slices without carbon peaks (grey lines in SDROSS figures) are used to determine the error bars for α and β carbons in figure 1 in the main text. The SDROSS profile of the acyl chain methyl carbons (left column) was used as reference assuming that these carbons have negative order parameters.

S6 Dihedral angle distributions of the headgroup and glycerol backbone regions of PS lipids from different simulation models

The dihedral angles and structures of the glycerol backbone and headgroup regions of POPS lipids show wide variety between different simulation models (Figs. S7, S8 and S9). Detailed discussion of the structural differences is limited by the lack of realistic model that would correctly reproduce the headgroup and glycerol backbone order parameters. However, some structural characteristics of PS headgroup can be suggested based on the best available models (Figs. S10, S11 and S12), as discussed in the main text. The glycerol backbone structures are not discussed in this work because our focus is on PS headgroup. However, the data presented here can be useful for future investigations.

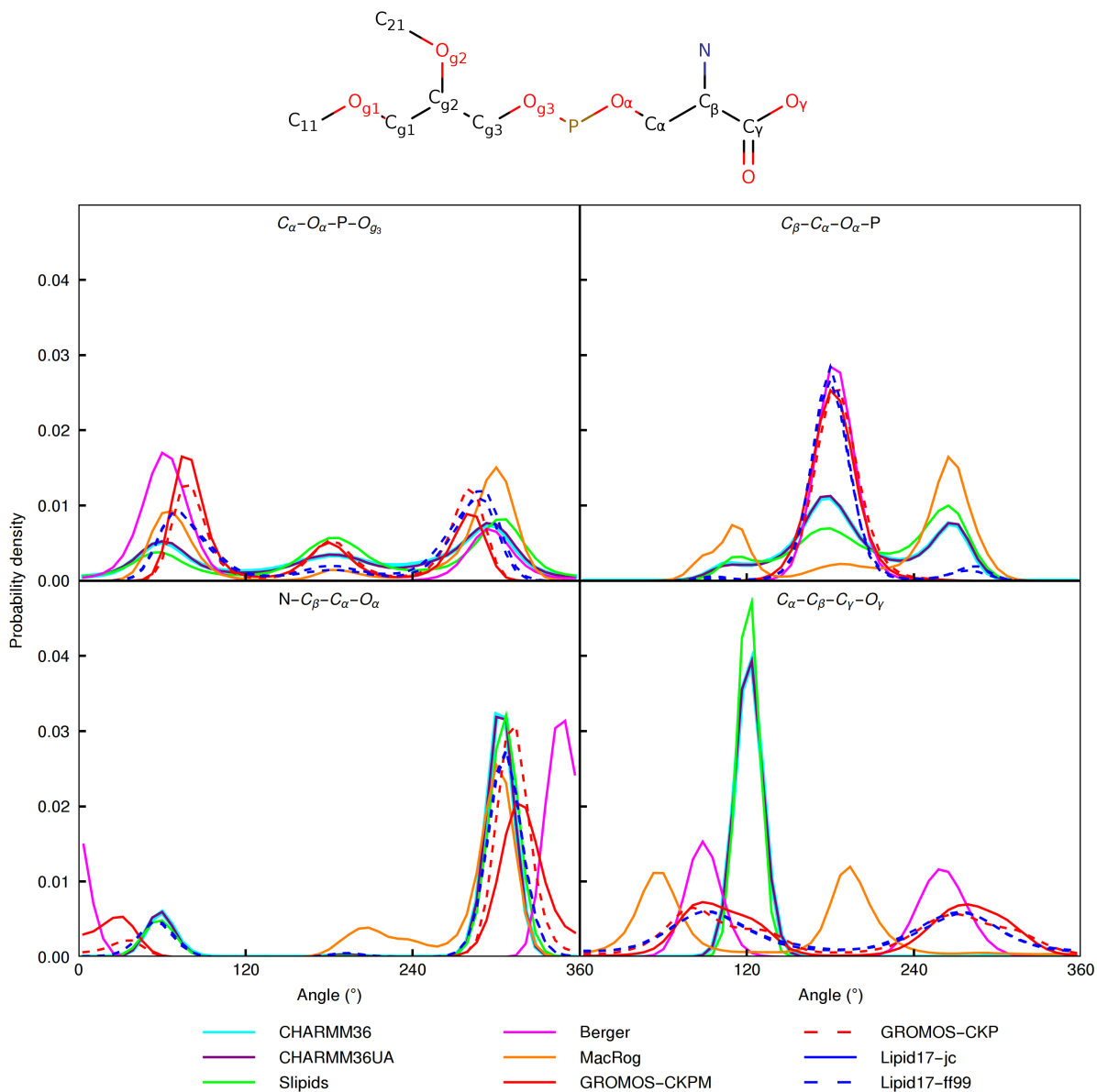


Figure S7: Dihedral angle distributions of the headgroup region of POPS from different simulation models.

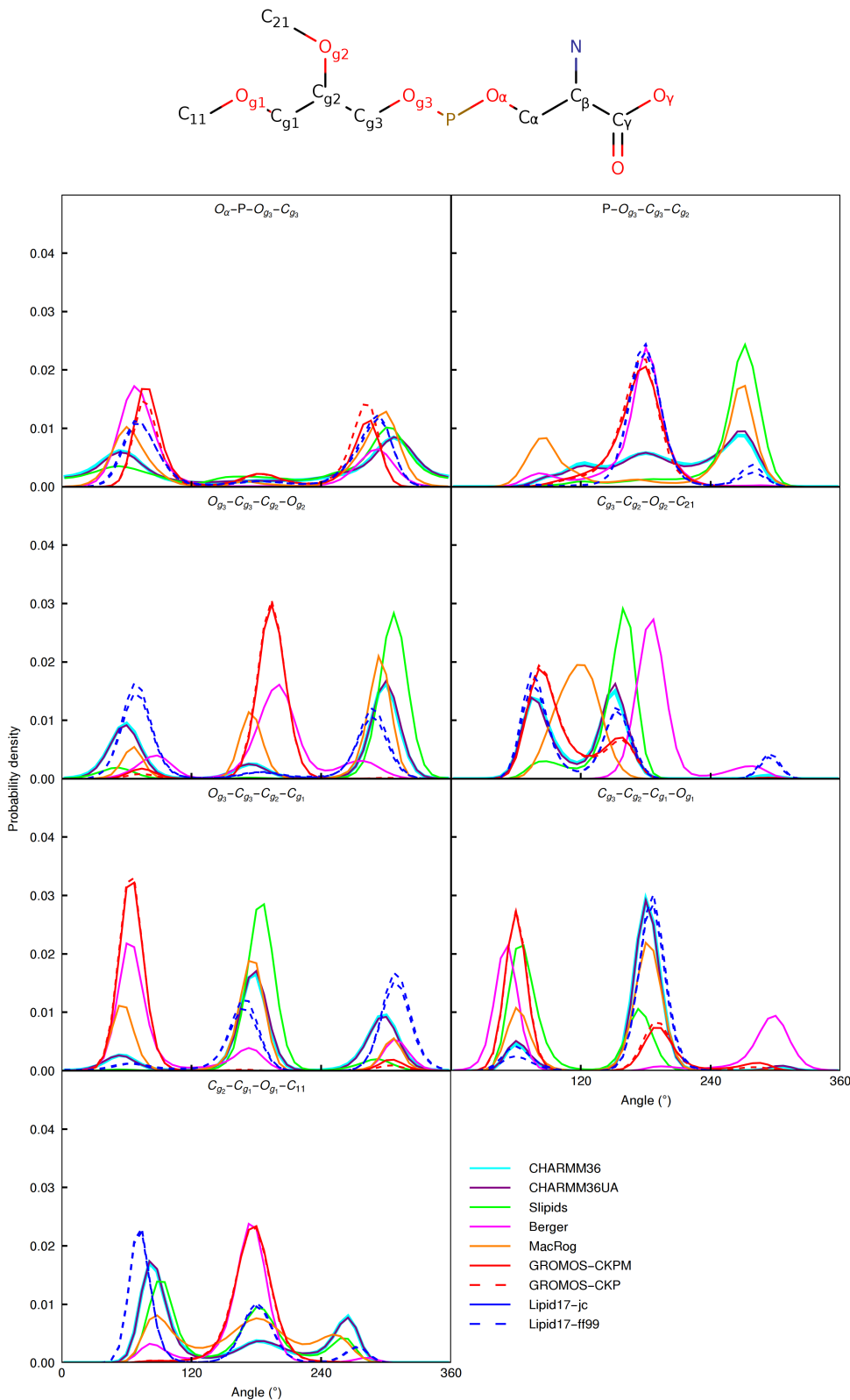


Figure S8: Dihedral angle distributions of the glycerol backbone region of POPS lipids from different simulation models.

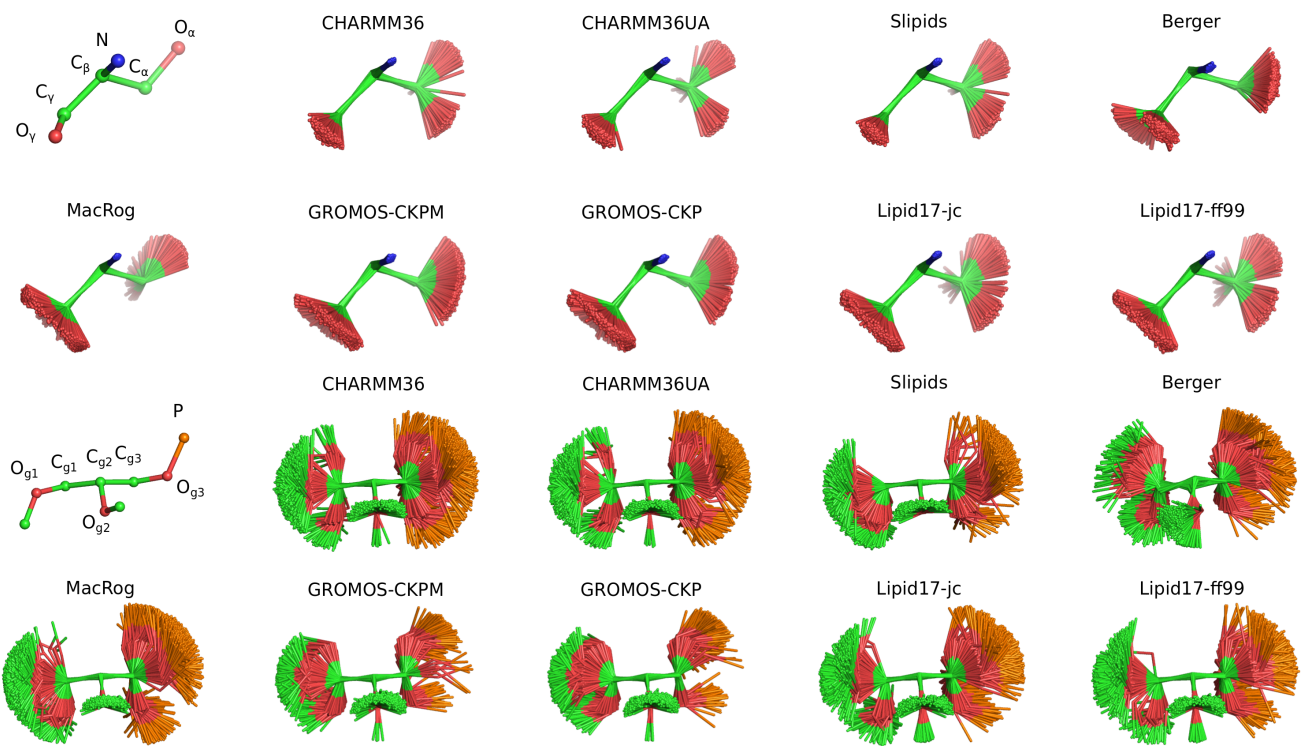


Figure S9: Overlayed snapshots of the glycerol backbone and headgroup regions from different POPS simulations.

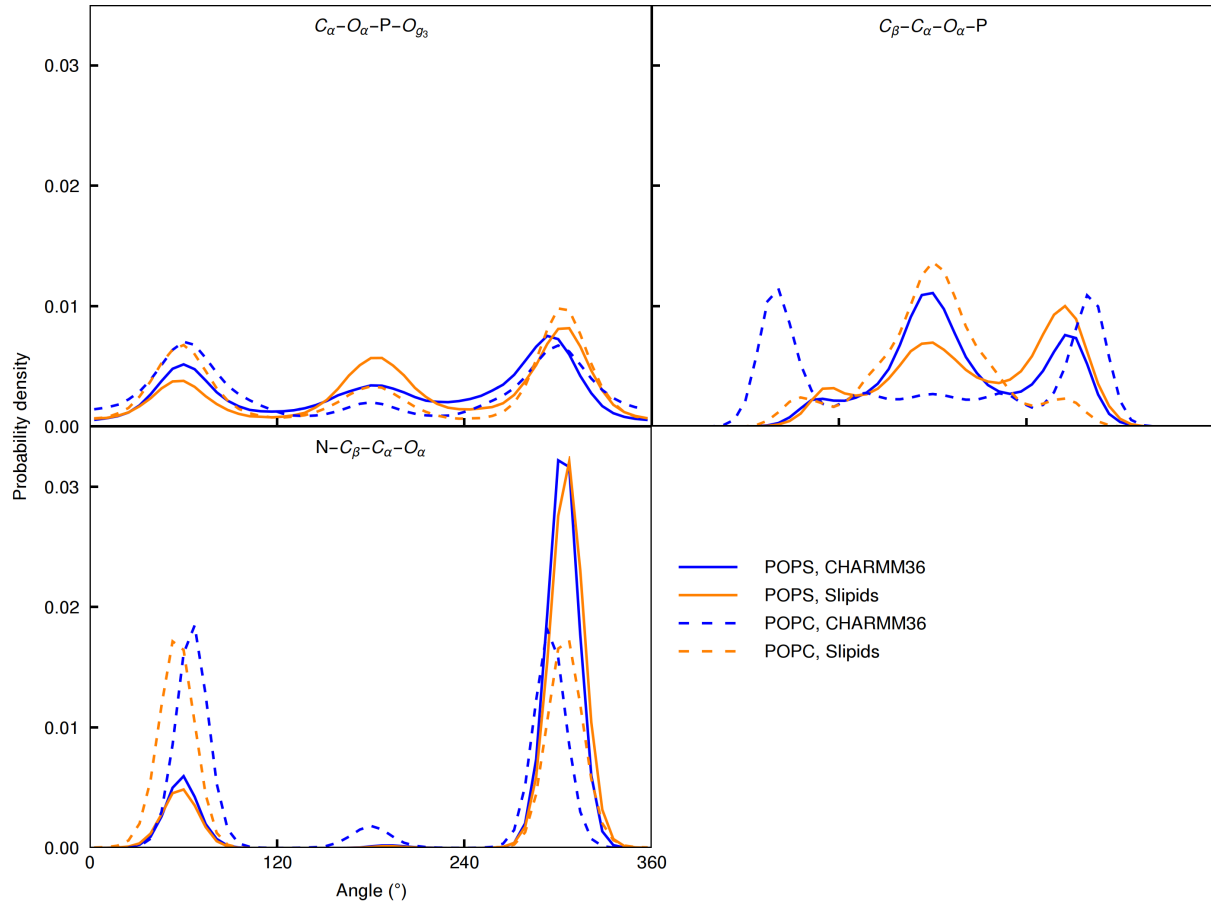


Figure S10: Dihedral angle distributions of the headgroup regions from CHARMM36 and Slipids simulations compared between the POPC and POPS lipids. The CHARMM36 POPC simulation is from Ref. 98 and Slipids POPC from Ref. 99.

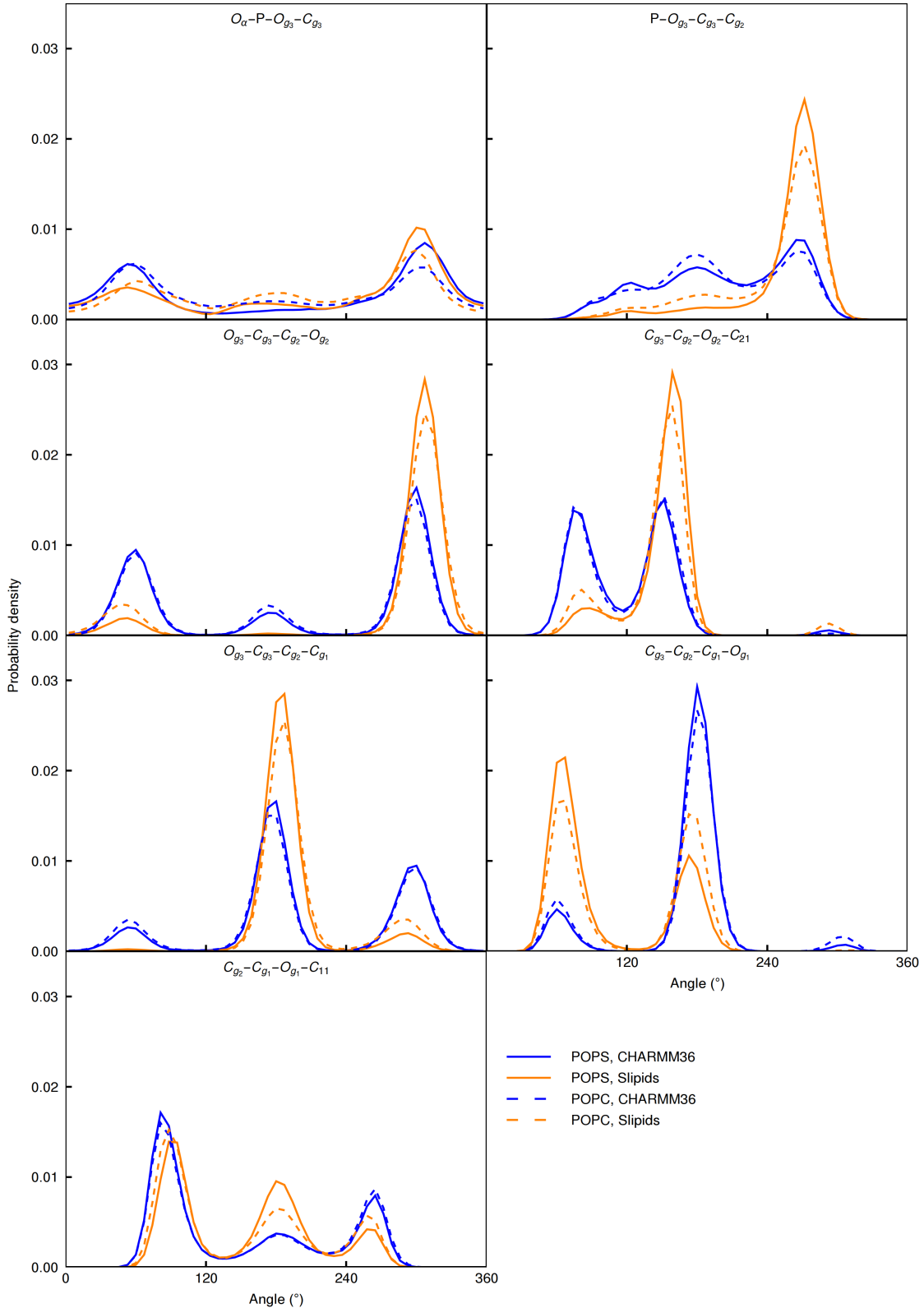


Figure S11: Dihedral angle distributions of the glycerol backbone regions from CHARMM36 and Slipids simulations compared between the POPC and POPS lipids. The CHARMM36 POPC simulation is from Ref. 98 and Slipids POPC from Ref. 99.

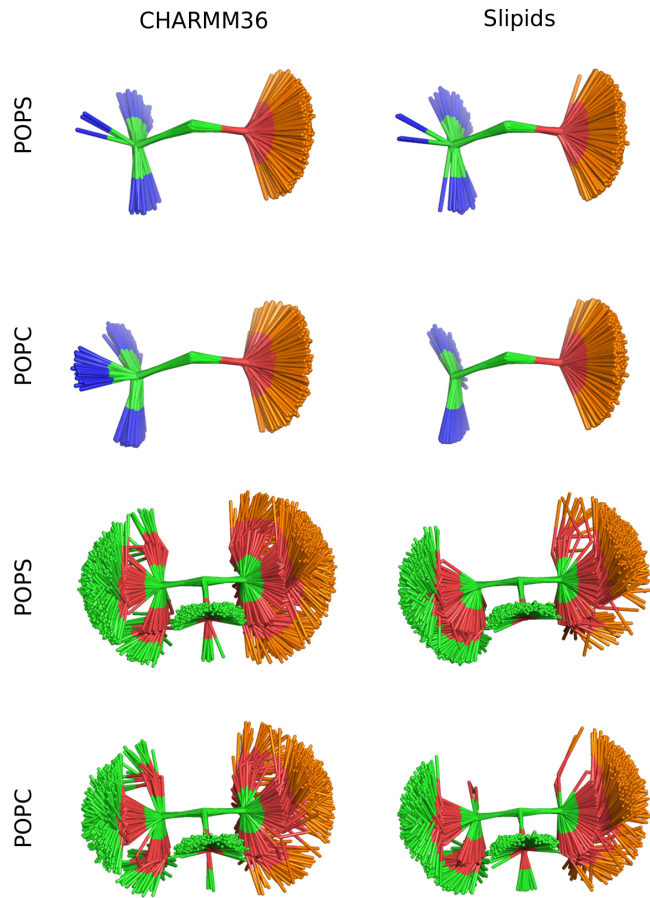


Figure S12: Overlayed snapshots of the headgroup and glycerol backbone regions from CHARMM36 and Slipids simulations compared between the POPC and POPS lipids. The CHARMM36 POPC simulation is from Ref. 98 and Slipids POPC from Ref. 99.

S7 Headgroup response to the additional counterions in POPC:POPS (5:1) mixtures

To evaluate counterion binding in different simulation models against experimental data,¹ we plot the headgroup order parameters measured from POPC:POPS 5:1 mixture as a function of different monovalent ions added to the buffer (Fig. S13). Experimental order parameters of POPC headgroup in the mixture are available as a function of LiCl and KCl concentrations, while POPS headgroup order parameters are measured also in increasing NaCl concentration. Lithium interacts more strongly with PS headgroups than other monovalent ions,^{1,87,100–102} as also observed for PC headgroups.¹⁰³ The different binding behaviour is evident based on the response of PS headgroup order parameters, which decrease with the addition of lithium but increase with the addition of sodium or potassium (Fig. S13). POPC headgroup order parameters exhibit a clear decrease as a function of LiCl concentration but only modest changes as a function of KCl concentration, indicating significant Li⁺ binding but only weak K⁺ binding to the mixture when interpreted using the electrometer concept.^{81–83}

In simulations with Berger and CHARMM36 models, the responses of POPC and POPS order parameter to added sodium and potassium are not in line with the experiments. Instead, the simulations produce a response similar to experiments conducted in LiCl (Fig. S13), indicating overestimated binding affinity of sodium and potassium in these simulations. The MacRog simulations with potassium exhibit weaker counterion binding affinity (Fig. S14), but significantly larger error bars and less systematic changes in the order parameters (Fig. S13). Similar unsystematic behaviour was also observed in the simulations of Lipid14/17 model with the additional counterions,^{16–19} for which the data is not shown due to the formation of ion clusters in water with relatively low (1 M) ion concentrations (Fig. S15). Appearance of such clusters in the MagRog simulations with 4 M KCl could explain the unsystematic changes of the order parameters in this model upon increasing KCl. In conclusion, the results are in line with the section in the main text, suggesting that the MacRog simulations with

KCl give the most realistic surface charge at the lipid bilayer interface among the tested simulation models.

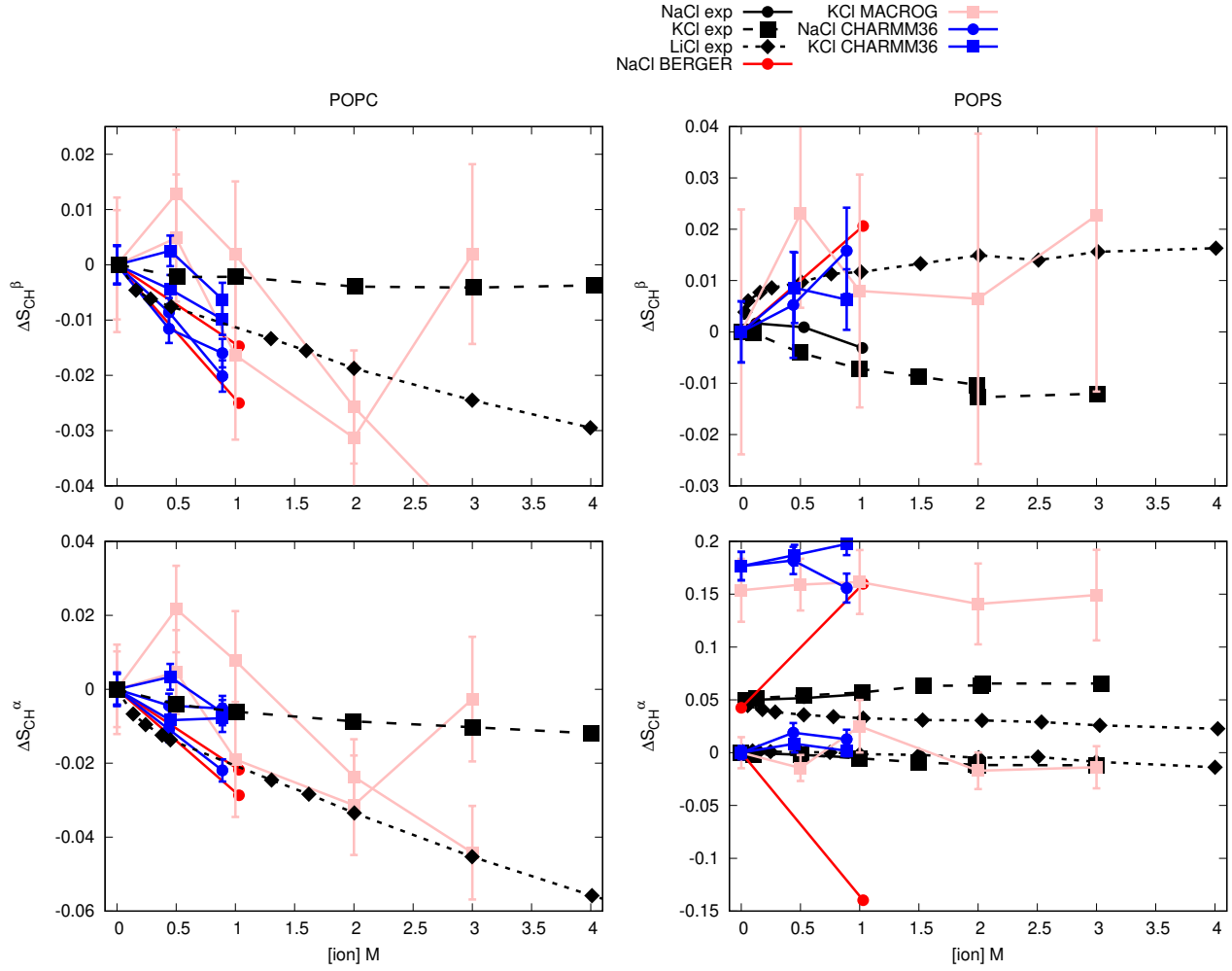


Figure S13: Changes of the PC (left) and PS (right) headgroup order parameters as a function of added NaCl, KCl and LiCl from POPC:POPS (5:1) mixture at 298 K (except Berger simulations are (4:1) mixture at 310 K). The experimental data is from Ref. 1. The values from counterion-only systems are set as a zero point of y-axis. To correctly illustrate the significant forking of the α -carbon order parameter in PS headgroup (bottom, right), the y-axis is shifted with the same value for both order parameters such that the lower order parameter value is at zero.

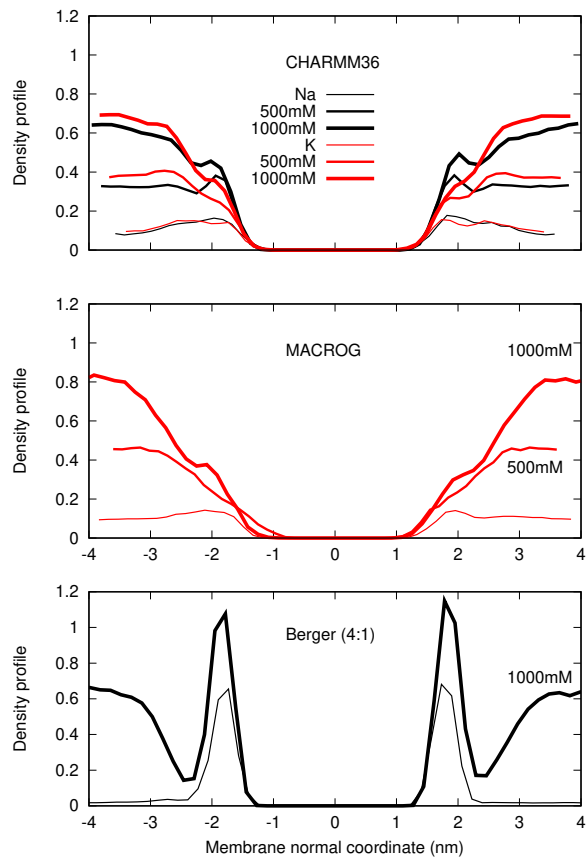


Figure S14: Counterion density distributions from PC:PS mixtures.

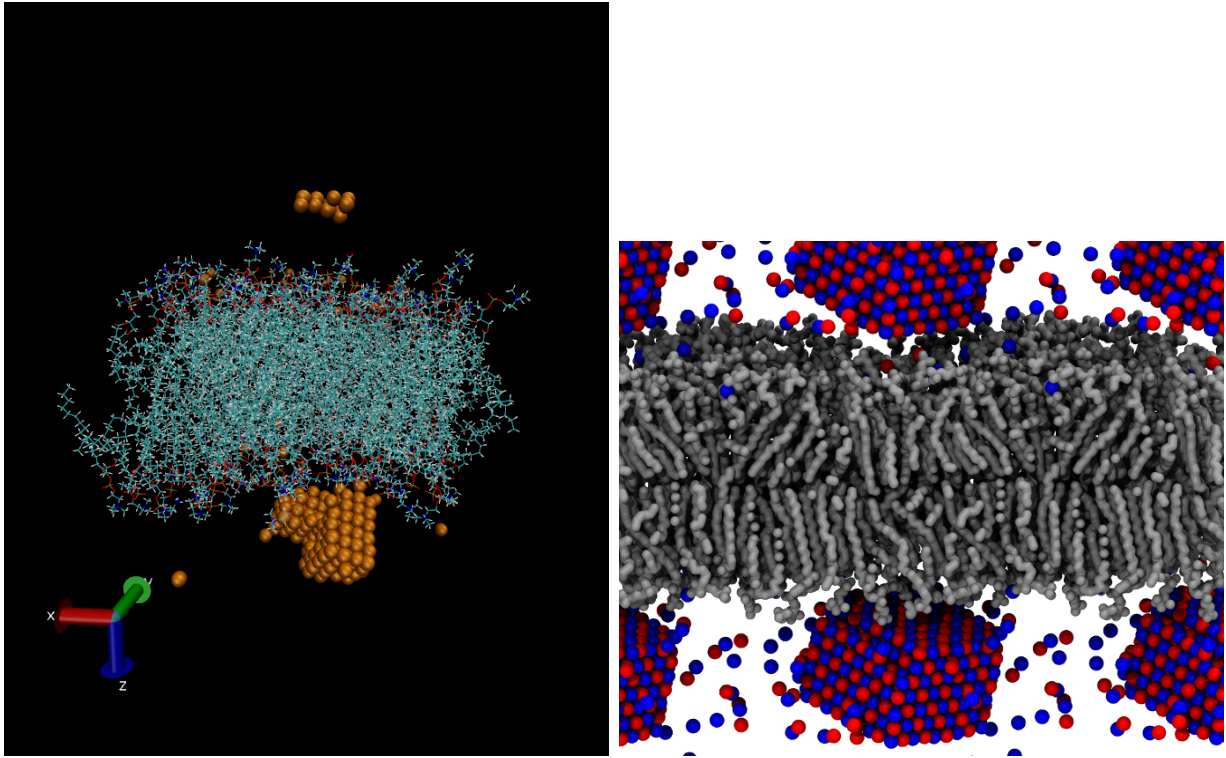


Figure S15: Ion clusters appearing in POPC:POPS (5:1) lipid17/14 simulations with 1 M of NaCl (left) and MacRog simulations with 4 M of KCl (right).

S8 Calcium binding to POPC in CHARMM36 simulation with NBfix

The response of POPC headgroup order parameters to the CaCl₂ concentration are underestimated in simulations of POPC:POPS (5:1) mixture with CHARMM36 when employing NBfix (as obtained from CHARMM-GUI in January 2018) for interactions between calcium and lipid oxygens¹⁰⁴ (Fig. 9 in the main text), indicating that the calcium binding to the bilayer is too weak with these parameters. The response of headgroup order parameters (Fig. S16) and the binding affinity (Fig. S17) of calcium also to a pure POPC bilayer are underestimated when using NBfix ions. Notably, CHARMM36 simulations with the NBfix terms^{3,104} predict similar binding affinity for sodium and calcium. Without the NBfix term, the calcium binding affinity to pure POPC lipid bilayers was overestimated in the CHARMM36 model.⁹³

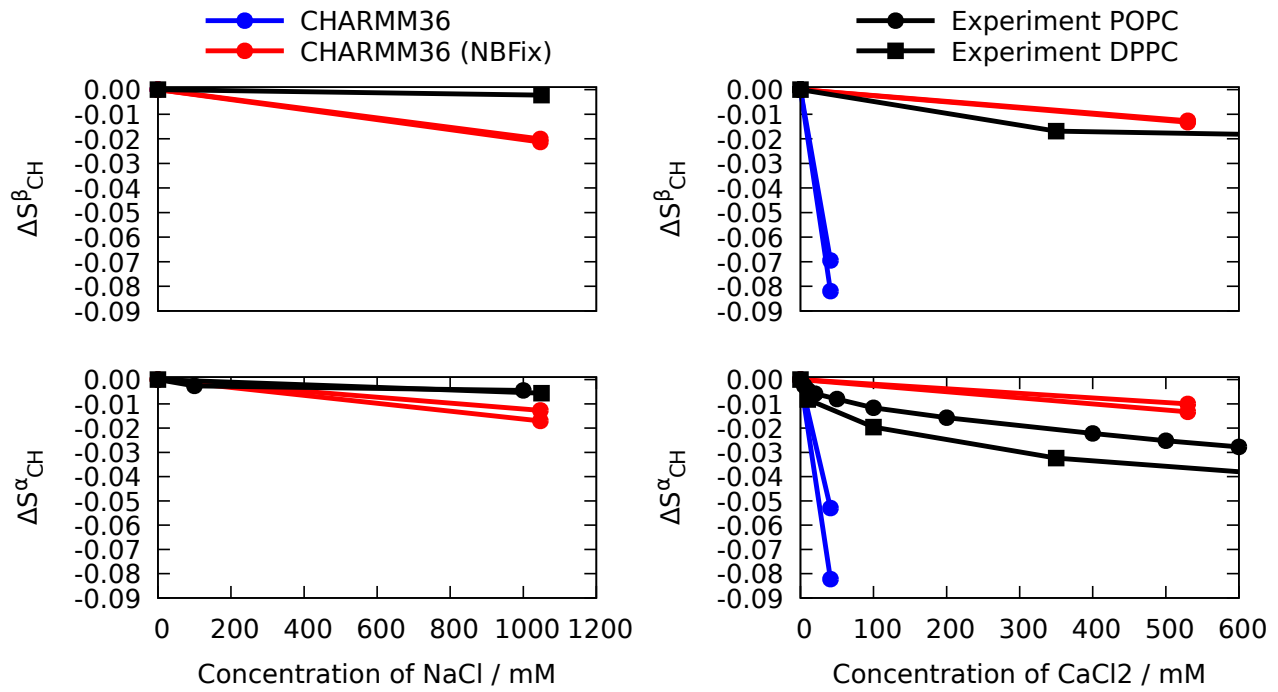


Figure S16: Headgroup order parameters from CHARMM36 simulations of POPC, where the NBfix term was employed for sodium³ (*left*) and calcium¹⁰⁴ (*right*) compared with the experimental data^{81,82} and simulations without NBfix for the calcium. Simulation files without ions are available at Ref. 105, with the NBfix term in sodium at Ref. 106, with the NBfix term in calcium at Ref. 106 and without the NBfix in calcium at Ref. 107.

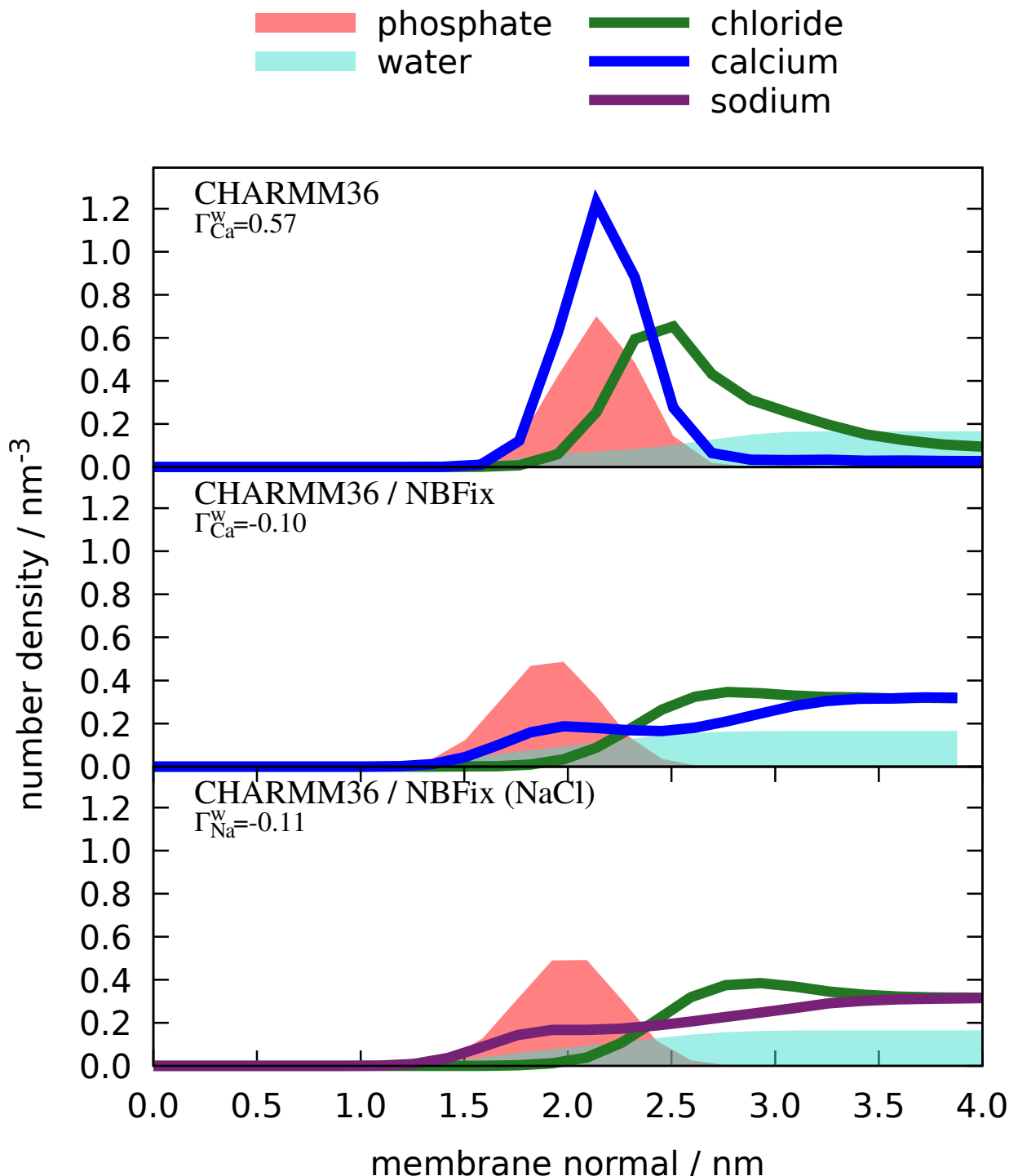


Figure S17: Density profiles along membrane normal from CHARMM36 simulations with (middle) and without (top) the NBfix term for calcium¹⁰⁴ compared to the simulation with the NBfix term for sodium³ (bottom). The simulation data are the same as in figure S16.

S9 Calcium density profiles from simulations with POPC:POPS(5:1) mixture

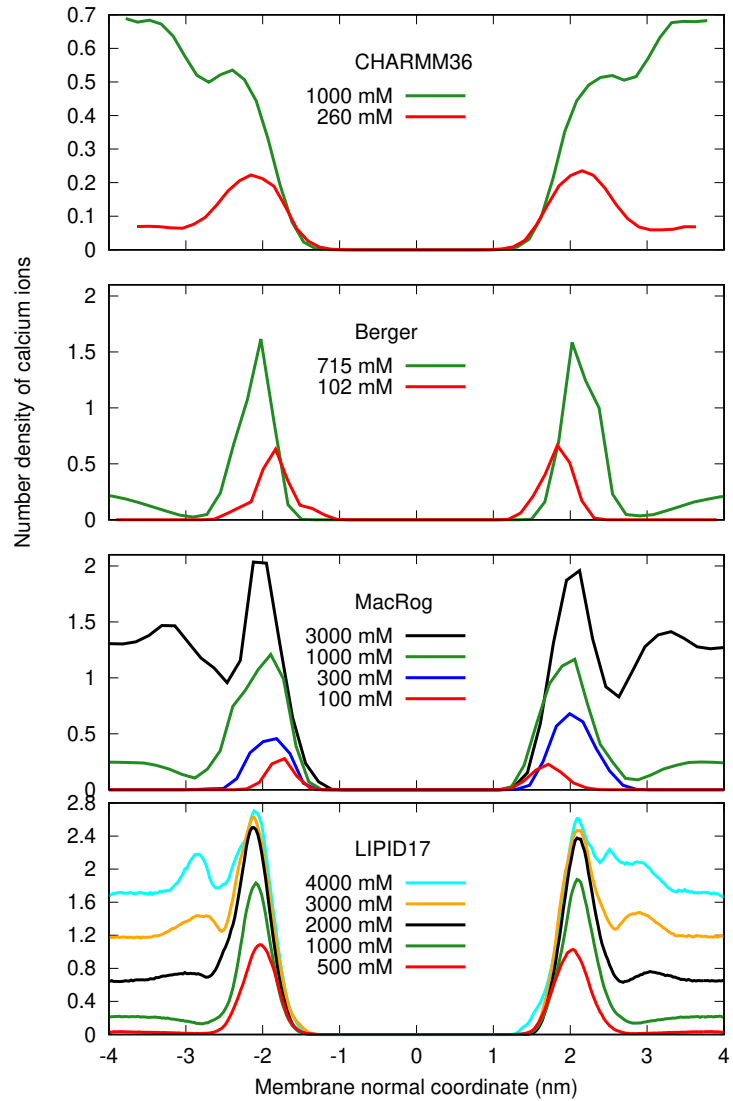


Figure S18: Number density profiles of Ca^{2+} from POPC:POPS (5:1) mixtures simulated with different force fields. The ion densities are taken along the z-axis that coincides with the bilayer normal.

S10 Details of the rough subjective force field ranking (Fig. 5)

S11 Details of the force field ranking (Fig. 5)

In Figure 3) of main text we present a rough and subjective ranking of the force fields investigated in this work. The assessment was based on the data presented in Fig. 3. For each carbon (the columns in Fig. 3), we first investigated separately how well a given force field represents the **magnitude** of the order parameters and their **forking**.

Magnitude

To quantify how close to the experimentally obtained C–H order parameters (S_{CHS}) were to the force-field-produced S_{CHS} , we assign a number for each carbon based on the following 5-step scale:

0 (): More than half of all the calculated S_{CHS} (includes all hydrogens bound to that carbon and all lipid types investigated for the given force field) were within the *subjective sweet spots* (SSP, blue-shaded areas in Fig. 3).

1 (m): All the calculated S_{CHS} were < 0.03 units away from the SSP.

2 (M): All the calculated S_{CHS} were < 0.05 units away from the SSP.

3 (M): All the calculated S_{CHS} were < 0.10 units away from the SSP.

4 (M): Some of the calculated S_{CHS} were > 0.10 units away from the SSP.

Forking

Forking in each force field was assessed based on how well the difference in order parameters of two hydrogens attached to a given carbon matched that obtained experimentally. Note

that this is not relevant for β and g_2 , which have only one hydrogen. For the α carbon, for which a considerable forking of 0.105 is experimentally seen, the following 5-step scale was used:

0 (): The distance D between the symbols (indicating time-weighted averages in Fig. 3) was $0.08 < D < 0.13$ units for all the calculated S_{CHs} (includes all lipid types investigated for a given force field).

1 (f): $(0.06 < D < 0.08)$ OR $(0.13 < D < 0.15)$.

2 (F): $(0.04 < D < 0.06)$ OR $(0.15 < D < 0.17)$.

3 (F): $(0.02 < D < 0.04)$ OR $(0.17 < D < 0.19)$.

4 (F): $(D < 0.02)$ OR $(0.19 < D)$.

For the g_3 carbon, for which no forking is indicated by experiments, the following 5-step scale was used:

0 (): $D < 0.02$.

1 (f): $0.02 < D < 0.04$.

2 (F): $0.04 < D < 0.06$.

3 (F): $0.06 < D < 0.08$.

4 (F): $0.08 < D$.

For the g_1 carbon, for which a considerable forking of 0.13 is experimentally seen, the following 5-step scale was used:

0 (): $0.11 < D < 0.15$.

1 (f): $(0.09 < D < 0.11)$ OR $(0.15 < D < 0.17)$.

2 (F): $(0.07 < D < 0.09)$ OR $(0.17 < D < 0.19)$.

3 (F): $(0.05 < D < 0.07)$ OR $(0.19 < D < 0.21)$.

4 (F): $(D < 0.05)$ OR $(0.21 < D)$.

Based on these assessments of magnitude and forking deviations from experimental values, each carbon was then assigned to one of the following groups: "within experimental error" (magnitude and forking deviations both on 0 of the scales described above), "almost within experimental error" (sum of the magnitude and forking deviation 1 or 2), "clear deviation from experiments" (sum of magnitude and forking deviation from 3 to 5), and "major deviation from experiments" (sum of magnitude and forking deviation from 6 to 8). These groups are indicated by colors in Fig. 4. (Note that for β and g_2 , for which there can be no forking, the corresponding group assignment limits were: 0, 1, 2, and 3.)

Finally, the total ability of the force field to describe the headgroup and glycerol structure was estimated. To this end, the groups were given the following weights: 0 (within experimental error), 1 (almost within experimental error), 2 (clear deviation from experiments), 4 (major deviation from experiments), and the contributions from the five carbons were summed up. The sum, given in the Σ -column of Fig. 3, was then used to (roughly and subjectively) rank the force fields.

S12 Author contributions

Hanne Antila Contributed to the development analysis tools used for evaluating the force fields, provided critical discussion on the manuscript content and edited it for clarity.

Pavel Buslaev

Fernando Favela

Tiago M. Ferreira

Ivan Gushchin

Matti Javanainen Performed most of the MacRog simulations and provided comments on the manuscript.

Batuhan Kav

Jesper J. Madsen

Josef Melcr

Markus Miettinen

Ricky Nencini

O. H. Samuli Ollila Designed the project and managed the work. Ran and analysed several simulations. Wrote the manuscript.

Thomas Piggot

References

- (1) Roux, M.; Bloom, M. Calcium, magnesium, lithium, sodium, and potassium distributions in the headgroup region of binary membranes of phosphatidylcholine and phosphatidylserine as seen by deuterium NMR. *Biochemistry* **1990**, *29*, 7077–7089.
- (2) Klauda, J. B.; Venable, R. M.; Freites, J. A.; O'Connor, J. W.; Tobias, D. J.; Mondragon-Ramirez, C.; Vorobyov, I.; MacKerell Jr, A. D.; Pastor, R. W. Update of the CHARMM All-Atom Additive Force Field for Lipids: Validation on Six Lipid Types. *J. Phys. Chem. B* **2010**, *114*, 7830–7843.
- (3) Venable, R. M.; Luo, Y.; Gawrisch, K.; Roux, B.; Pastor, R. W. Simulations of Anionic Lipid Membranes: Development of Interaction-Specific Ion Parameters and Validation Using NMR Data. *The Journal of Physical Chemistry B* **2013**, *117*, 10183–10192.
- (4) Madsen, J. J. MD simulations of bilayers containing PC/PS mixtures and CaCl₂:150POPC_150POPS_neutral. 2019; <https://doi.org/10.5281/zenodo.2542164>.
- (5) Piggot, T. CHARMM36 POPS/POPC simulations (versions 1 and 2) 298 K 1.0 nm LJ switching with K ions. 2018; <https://doi.org/10.5281/zenodo.1182658>.
- (6) Ollila, O. H. S. POPC:POPS (5:1) with 450 mM potassium simulation with CHARMM36 at 298K. 2018; <https://doi.org/10.5281/zenodo.1493241>.
- (7) Ollila, O. H. S. POPC:POPS (5:1) with 890 mM potassium simulation with CHARMM36 at 298K. 2018; <https://doi.org/10.5281/zenodo.1493246>.
- (8) Piggot, T. CHARMM36 POPS/POPC simulations (versions 1 and 2) 298 K 1.0 nm LJ switching with Na ions. 2018; <https://doi.org/10.5281/zenodo.1182665>.
- (9) Ollila, O. H. S. POPC:POPS (5:1) with 440 mM sodium simulation with CHARMM36 at 298K. 2018; <https://doi.org/10.5281/zenodo.1493190>.

- (10) Ollila, O. H. S. POPC:POPS (5:1) with 890 mM sodium simulation with CHARMM36 at 298K. 2018; <https://doi.org/10.5281/zenodo.1493229>.
- (11) Maciejewski, A.; Pasenkiewicz-Gierula, M.; Cramariuc, O.; Vattulainen, I.; Rög, T. Refined OPLS All-Atom Force Field for Saturated Phosphatidylcholine Bilayers at Full Hydration. *J. Phys. Chem. B* **2014**, *118*, 4571–4581.
- (12) Javanainen, M. Simulations of POPC/POPS membranes with CaCl₂. 2017; <https://doi.org/10.5281/zenodo.1409551>.
- (13) Javanainen, M. Simulations of POPC/POPS membranes with KCl. 2018; <https://doi.org/10.5281/zenodo.1404040>.
- (14) Dickson, C. J.; Madej, B. D.; Skjevik, A. A.; Betz, R. M.; Teigen, K.; Gould, I. R.; Walker, R. C. Lipid14: The Amber Lipid Force Field. *J. Chem. Theory Comput.* **2014**, *10*, 865–879.
- (15) Gould, I.; Skjevik, A.; Dickson, C.; Madej, B.; Walker, R. Lipid17: A Comprehensive AMBER Force Field for the Simulation of Zwitterionic and Anionic Lipids. 2018; In preparation.
- (16) Kav, B.; Miettinen, M. S. Amber Lipid17 Simulations of POPC/POPS Membranes with KCl Counterions. 2018; <https://doi.org/10.5281/zenodo.1250969>, B.K acknowledges financial support from International Max Planck Research School on Multiscale Bio-Systems.
- (17) Kav, B.; Miettinen, M. S. Amber Lipid17 Simulations of POPC/POPS Membranes with KCl. 2018; <https://doi.org/10.5281/zenodo.1227257>, B.K acknowledges financial support from International Max Planck Research School on Multiscale Bio-Systems.
- (18) Kav, B.; Miettinen, M. S. Amber Lipid17 Simulations of POPC/POPS Membranes with NaCl Counterions. 2018; <https://doi.org/10.5281/zenodo.1250975>, B.K acknowl-

edges financial support from International Max Planck Research School on Multiscale Bio-Systems.

- (19) Kav, B.; Miettinen, M. S. Amber Lipid17 Simulations of POPC/POPS Membranes with NaCl. 2018; <https://doi.org/10.5281/zenodo.1227272>, B.K acknowledges financial support from International Max Planck Research School on Multiscale Bio-Systems.
- (20) Tielemans, D. P.; Berendsen, H. J.; Sansom, M. S. An Alamethicin Channel in a Lipid Bilayer: Molecular Dynamics Simulations. *Biophys. J.* **1999**, *76*, 1757 – 1769.
- (21) Mukhopadhyay, P.; Monticelli, L.; Tielemans, D. P. Molecular Dynamics Simulation of a Palmitoyl-Oleoyl Phosphatidylserine Bilayer with Na⁺ Counterions and NaCl. *Biophysical Journal* **2004**, *86*, 1601 – 1609.
- (22) Samuli, O. O. H. POPC:POPS (4:1) simulation with Berger model at 310K. 2018; <https://doi.org/10.5281/zenodo.1475285>.
- (23) Cwiklik, L. MD simulation trajectory of a POPC/POPS (4:1) bilayer with 1M NaCl, Berger force field for lipids and ffgmx for ions. 2017; <https://doi.org/10.5281/zenodo.838219>.
- (24) Botan, A.; Favela-Rosales, F.; Fuchs, P. F. J.; Javanainen, M.; Kanduč, M.; Kulig, W.; Lamberg, A.; Loison, C.; Lyubartsev, A.; Miettinen, M. S. et al. Toward Atomistic Resolution Structure of Phosphatidylcholine Headgroup and Glycerol Backbone at Different Ambient Conditions. *J. Phys. Chem. B* **2015**, *119*, 15075–15088.
- (25) Fernando, F.-R. POPC_Glycerol_CHARMM36_0-10-15-20-25-35-50%CHOL. 2015; <http://dx.doi.org/10.5281/zenodo.16830>, Because of the system size, the files ONLY contain the coordinates of Glycerol saved every 10ps, this is the real contribution to the nmrlipids project.

- (26) Piggot, T. CHARMM36 DOPS simulations (versions 1 and 2) 303 K 1.0 nm LJ switching. 2017; <https://doi.org/10.5281/zenodo.1129411>.
- (27) Piggot, T. CHARMM36 POPS simulations (versions 1 and 2) 298 K 1.0 nm LJ switching. 2017; <https://doi.org/10.5281/zenodo.1129415>.
- (28) Piggot, T. CHARMM36 POPS simulations (versions 1 and 2) 298 K 1.0 nm LJ switching with K ions. 2018; <https://doi.org/10.5281/zenodo.1182654>.
- (29) Madsen, J. J. MD simulations of bilayers containing PC/PS mixtures and CaCl₂: 250POPC_50POPS_neutral. 2019; <https://doi.org/10.5281/zenodo.2542151>.
- (30) Lee, J.; Cheng, X.; Swails, J. M.; Yeom, M. S.; Eastman, P. K.; Lemkul, J. A.; Wei, S.; Buckner, J.; Jeong, J. C.; Qi, Y. et al. CHARMM-GUI Input Generator for NAMD, GROMACS, AMBER, OpenMM, and CHARMM/OpenMM Simulations Using the CHARMM36 Additive Force Field. *Journal of Chemical Theory and Computation* **2016**, *12*, 405–413.
- (31) Jo, S.; Kim, T.; Iyer, V. G.; Im, W. CHARMM-GUI: A web-based graphical user interface for CHARMM. *Journal of Computational Chemistry* **29**, 1859–1865.
- (32) Abraham, M. J.; Murtola, T.; Schulz, R.; Páll, S.; Smith, J. C.; Hess, B.; Lindahl, E. GROMACS: High performance molecular simulations through multi-level parallelism from laptops to supercomputers. *SoftwareX* **2015**, *1*, 19–25.
- (33) Madsen, J. J. MD simulations of bilayers containing PC/PS mixtures and CaCl₂: 250POPC_50POPS_0.15M_{CaCl}₂. 2019; <https://doi.org/10.5281/zenodo.2542176>.
- (34) Madsen, J. J. MD simulations of bilayers containing PC/PS mixtures and CaCl₂: 250POPC_50POPS_1M_{CaCl}₂. 2019; <https://doi.org/10.5281/zenodo.2542135>.

- (35) Piggot, T. CHARMM36-UA DOPS simulations (versions 1 and 2) 303 K 1.0 nm LJ switching. 2017; <https://doi.org/10.5281/zenodo.1129456>.
- (36) Piggot, T. CHARMM36-UA POPS simulations (versions 1 and 2) 298 K 1.0 nm LJ switching. 2017; <https://doi.org/10.5281/zenodo.1129458>.
- (37) Kulig, W.; Pasenkiewicz-Gierula, M.; Róg, T. Topologies, structures and parameter files for lipid simulations in GROMACS with the OPLS-aa force field: DPPC, POPC, DOPC, PEPC, and cholesterol. *Data in Brief* **2015**, *5*, 333 – 336.
- (38) Kulig, W.; Pasenkiewicz-Gierula, M.; Róg, T. Cis and trans unsaturated phosphatidyl-choline bilayers: A molecular dynamics simulation study. *Chem. Phys. Lipids* **2016**, *195*, 12 – 20.
- (39) Jorgensen, W. L.; Chandrasekhar, J.; Madura, J. D.; Impey, R. W.; Klein, M. L. Comparison of simple potential functions for simulating liquid water. *J. Chem. Phys.* **1983**, *79*, 926–935.
- (40) Javanainen, M. Simulation of a POPC bilayer at 298K, lipid model by Maciejewski and Rog. 2018; <https://doi.org/10.5281/zenodo.1167532>.
- (41) Piggot, T. MacRog POPS simulations (versions 1 and 2) 298 K with corrected PO not OP tails. 2018; <https://doi.org/10.5281/zenodo.1283335>.
- (42) Javanainen, M. Simulation of a POPS membrane with potassium counterions. 2018; <https://doi.org/10.5281/zenodo.1434990>.
- (43) Åqvist, J. Ion-water interaction potentials derived from free energy perturbation simulations. *J. Phys. Chem.* **1990**, *94*, 8021–8024.
- (44) Róg, T.; Orłowski, A.; Llorente, A.; Skotland, T.; Sylvänen, T.; Kauhanen, D.; Ekroos, K.; Sandvig, K.; Vattulainen, I. Data including GROMACS input files for atomistic molecular dynamics simulations of mixed, asymmetric bilayers including

molecular topologies, equilibrated structures, and force field for lipids compatible with OPLS-AA parameters. *Data in Brief* **2016**, *7*, 1171 – 1174.

- (45) Essman, U. L.; Perera, M. L.; Berkowitz, M. L.; Larden, T.; Lee, H.; Pedersen, L. G. A smooth particle mesh ewald potential. *J. Chem. Phys.* **1995**, *103*, 8577–8592.
- (46) Shirts, M. R.; Mobley, D. L.; Chodera, J. D.; Pande, V. S. Accurate and Efficient Corrections for Missing Dispersion Interactions in Molecular Simulations. *The Journal of Physical Chemistry B* **2007**, *111*, 13052–13063.
- (47) Nose, S. A molecular dynamics method for simulations in the canonical ensemble. *Mol. Phys.* **1984**, *52*, 255–268.
- (48) Hoover, W. G. Canonical dynamics: Equilibrium phase-space distributions. *Phys. Rev. A* **1985**, *31*, 1695–1697.
- (49) Parrinello, M.; Rahman, A. Polymorphic transitions in single crystals: A new molecular dynamics method. *J. Appl. Phys.* **1981**, *52*, 7182–7190.
- (50) Hess, B.; Bekker, H.; Berendsen, H. J. C.; Fraaije, J. G. E. M. LINCS: a linear constraint solver for molecular dynamics simulations. *J. Comput. Chem.* **1997**, *18*, 1463–1472.
- (51) Hess, B. P-LINCS: A Parallel Linear Constraint Solver for Molecular Simulation. *J. Chem. Theory Comput.* **2008**, *4*, 116–122.
- (52) Miyamoto, S.; Kollman, P. A. SETTLE: An analytical Version of the SHAKE and RATTLE Algorithm for Rigid Water Models. *J. Comput. Chem.* **1992**, *13*, 952–962.
- (53) Jorgensen, W. L.; Chandrasekhar, J.; Madura, J. D.; Impey, R. W.; Klein, M. L. Comparison of simple potential functions for simulating liquid water. *The Journal of chemical physics* **1983**, *79*, 926–935.
- (54) Case, D.; Ben-Shalom, I.; Brozell, S.; Cerutti, D.; T.E. Cheatham, I.; Cruzeiro, V.; Darden, T.; Duke, R.; Ghoreishi, D.; Gilson, M. et al. AMBER 2018. 2018.

- (55) Joung, I. S.; Cheatham III, T. E. Determination of alkali and halide monovalent ion parameters for use in explicitly solvated biomolecular simulations. *The journal of physical chemistry B* **2008**, *112*, 9020–9041.
- (56) Miettinen, M. S.; Kav, B. Molecular dynamics simulation trajectory of an anionic lipid bilayer: 100 mol% POPS with Na⁺ counterions using Joung-Cheatham Ions. 2018; <https://doi.org/10.5281/zenodo.1148495>, B.K. acknowledges financial support from International Max Planck Research School on Multiscale Bio-Systems.
- (57) Miettinen, M. S.; Kav, B. Molecular dynamics simulation trajectory of an anionic lipid bilayer: 100 mol% POPS with Na⁺ counterions using ff99 ions. 2018; <https://doi.org/10.5281/zenodo.1134869>, B.K. acknowledges financial support from International Max Planck Research School on Multiscale Bio-Systems.
- (58) Kav, B.; Miettinen, M. S. Molecular dynamics simulation trajectory of an anionic lipid bilayer: 100 mol% DOPS with Na⁺ counterions using Joung-Cheetham Ions. 2018; <https://doi.org/10.5281/zenodo.1134871>, B.K acknowledges financial support from International Max Planck Research School on Multiscale Bio-Systems.
- (59) Kav, B.; Miettinen, M. S. Molecular dynamics simulation trajectory of an anionic lipid bilayer: 100 mol% DOPS with Na⁺ counterions using ff99 Ions. 2018; <https://doi.org/10.5281/zenodo.1135142>, B.K acknowledges financial support from International Max Planck Research School on Multiscale Bio-Systems.
- (60) Kav, B.; Miettinen, M. S. Amber Lipid17 Simulations of POPC/POPS Membranes with CaCl₂. 2018; <https://doi.org/10.5281/zenodo.1438848>, B.K acknowledges financial support from International Max Planck Research School on Multiscale Bio-Systems.
- (61) Piggot, T. Slipids POPS simulations (versions 1 and 2) 298 K 1.0 nm cut-off with LJ-PME. 2017; <https://doi.org/10.5281/zenodo.1129441>.

- (62) Piggot, T. Slipids DOPS simulations (versions 1 and 2) 303 K 1.0 nm cut-off with LJ-PME. 2017; <https://doi.org/10.5281/zenodo.1129439>.
- (63) Ghahremanpour, M. M.; Arab, S. S.; Aghazadeh, S. B.; Zhang, J.; van der Spoel, D. MemBuilder: a web-based graphical interface to build heterogeneously mixed membrane bilayers for the GROMACS biomolecular simulation program. *Bioinformatics* **2013**, *30*, 439–441.
- (64) Jämbeck, J. P. M.; Lyubartsev, A. P. Derivation and Systematic Validation of a Refined All-Atom Force Field for Phosphatidylcholine Lipids. *J. Phys. Chem. B* **2012**, *116*, 3164–3179.
- (65) Jämbeck, J. P.; Lyubartsev, A. P. Another piece of the membrane puzzle: extending lipids further. *Journal of chemical theory and computation* **2012**, *9*, 774–784.
- (66) Darden, T.; York, D.; Pedersen, L. Particle mesh Ewald: An N·log(N) method for Ewald sums in large systems. *J. Chem. Phys.* **1993**, *98*, 10089–10092.
- (67) Ollila, S.; Hyvönen, M. T.; Vattulainen, I. Polyunsaturation in Lipid Membranes: Dynamic Properties and Lateral Pressure Profiles. *J. Phys. Chem. B* **2007**, *111*, 3139–3150.
- (68) Ollila, O. H. S. MD simulation of POPC lipids bilayer at 310K (Berger, Gromacs 3.1.4). 2018; <https://doi.org/10.5281/zenodo.1230170>.
- (69) Piggot, T. Berger POPS simulations (versions 1 and 2) 298 K 1.0 nm cut-off. 2017; <https://doi.org/10.5281/zenodo.1129425>.
- (70) Piggot, T. Berger DOPS simulations (versions 1 and 2) 303 K 1.0 nm cut-off. 2017; <https://doi.org/10.5281/zenodo.1129419>.
- (71) Jurkiewicz, P.; Cwiklik, L.; Vojtíšková, A.; Jungwirth, P.; Hof, M. Structure, dynamics,

and hydration of POPC/POPS bilayers suspended in NaCl, KCl, and CsCl solutions.

Biochimica et Biophysica Acta (BBA) - Biomembranes **2012**, *1818*, 609 – 616.

- (72) Melcrová, A.; Pokorna, S.; Pullanchery, S.; Kohagen, M.; Jurkiewicz, P.; Hof, M.; Jungwirth, P.; Cremer, P. S.; Cwiklik, L. The complex nature of calcium cation interactions with phospholipid bilayers. *Sci. Reports* **2016**, *6*, 38035.
- (73) Lukasz, C. MD simulation trajectory of a POPC/POPS (4:1) bilayer with 102mM CaCl₂, Berger force field for lipids, scaled charges for Ca²⁺ and Cl⁻. 2017; <https://doi.org/10.5281/zenodo.887398>.
- (74) Lukasz, C. MD simulation trajectory of a POPC/POPS (4:1) bilayer with 715mM CaCl₂, Berger force field for lipids, scaled charges for Ca²⁺ and Cl⁻. 2017; <https://doi.org/10.5281/zenodo.887400>.
- (75) Piggot, T. GROMOS-CKP POPS simulations (versions 1 and 2) 298 K with Berger/Chiu NH₃ charges and PME. 2017; <https://doi.org/10.5281/zenodo.1129431>.
- (76) Piggot, T. GROMOS-CKP POPS simulations (versions 1 and 2) 298 K with GROMOS NH₃ charges and PME. 2017; <https://doi.org/10.5281/zenodo.1129435>.
- (77) Piggot, T. GROMOS-CKP DOPS simulations (versions 1 and 2) 303 K with Berger/Chiu NH₃ charges and PME. 2017; <https://doi.org/10.5281/zenodo.1129429>.
- (78) Piggot, T. GROMOS-CKP DOPS simulations (versions 1 and 2) 303 K with GROMOS NH₃ charges and PME. 2017; <https://doi.org/10.5281/zenodo.1129447>.
- (79) Piggot, T. GROMOS-CKP POPS/POPC simulations (versions 1 and 2) 298 K with GROMOS NH₃ charges and PME. 2018; <https://doi.org/10.5281/zenodo.1283333>.

- (80) Piggot, T. GROMOS-CKP POPS/POPC simulations (versions 1 and 2) 298 K with Berger/Chiu NH₃ charges and PME. 2018; <https://doi.org/10.5281/zenodo.1283331>.
- (81) Akutsu, H.; Seelig, J. Interaction of metal ions with phosphatidylcholine bilayer membranes. *Biochemistry* **1981**, *20*, 7366–7373.
- (82) Altenbach, C.; Seelig, J. Calcium binding to phosphatidylcholine bilayers as studied by deuterium magnetic resonance. Evidence for the formation of a calcium complex with two phospholipid molecules. *Biochemistry* **1984**, *23*, 3913–3920.
- (83) Seelig, J.; MacDonald, P. M.; Scherer, P. G. Phospholipid head groups as sensors of electric charge in membranes. *Biochemistry* **1987**, *26*, 7535–7541.
- (84) Scherer, P. G.; Seelig, J. Electric charge effects on phospholipid headgroups. Phosphatidylcholine in mixtures with cationic and anionic amphiphiles. *Biochemistry* **1989**, *28*, 7720–7728.
- (85) Borle, F.; Seelig, J. Ca²⁺ binding to phosphatidylglycerol bilayers as studied by differential scanning calorimetry and ²H- and ³¹P-nuclear magnetic resonance. *Chemistry and Physics of Lipids* **1985**, *36*, 263 – 283.
- (86) Macdonald, P. M.; Seelig, J. Calcium binding to mixed phosphatidylglycerol-phosphatidylcholine bilayers as studied by deuterium nuclear magnetic resonance. *Biochemistry* **1987**, *26*, 1231–1240.
- (87) Roux, M.; Neumann, J.-M. Deuterium NMR study of head-group deuterated phosphatidylserine in pure and binary phospholipid bilayers. *FEBS Letters* **1986**, *199*, 33–38.
- (88) Roux, M.; Bloom, M. Calcium binding by phosphatidylserine headgroups. Deuterium NMR study. *Biophys. J.* **1991**, *60*, 38 – 44.

- (89) Scherer, P.; Seelig, J. Structure and dynamics of the phosphatidylcholine and the phosphatidylethanolamine head group in L-M fibroblasts as studied by deuterium nuclear magnetic resonance. *EMBO J.* **1987**, *6*.
- (90) Ferreira, T. M.; Coreta-Gomes, F.; Ollila, O. H. S.; Moreno, M. J.; Vaz, W. L. C.; Topgaard, D. Cholesterol and POPC segmental order parameters in lipid membranes: solid state ^1H - ^{13}C NMR and MD simulation studies. *Phys. Chem. Chem. Phys.* **2013**, *15*, 1976–1989.
- (91) Ollila, O. S.; Pabst, G. Atomistic resolution structure and dynamics of lipid bilayers in simulations and experiments. *Biochimica et Biophysica Acta (BBA) - Biomembranes* **2016**, *1858*, 2512 – 2528.
- (92) Ferreira, T. M.; Sood, R.; Bärenwald, R.; Carlström, G.; Topgaard, D.; Saalwächter, K.; Kinnunen, P. K. J.; Ollila, O. H. S. Acyl Chain Disorder and Azelaoyl Orientation in Lipid Membranes Containing Oxidized Lipids. *Langmuir* **2016**, *32*, 6524–6533.
- (93) Catte, A.; Girych, M.; Javanainen, M.; Loison, C.; Melcr, J.; Miettinen, M. S.; Monticelli, L.; Maatta, J.; Oganesyan, V. S.; Ollila, O. H. S. et al. Molecular electrometer and binding of cations to phospholipid bilayers. *Phys. Chem. Chem. Phys.* **2016**, *18*, 32560–32569.
- (94) Melcr, J.; Martinez-Seara, H.; Nencini, R.; Kolafa, J.; Jungwirth, P.; Ollila, O. H. S. Accurate Binding of Sodium and Calcium to a POPC Bilayer by Effective Inclusion of Electronic Polarization. *The Journal of Physical Chemistry B* **2018**, *122*, 4546–4557.
- (95) Ollila, O. H. S. CHARMM36 simulations of POPC mixed with cationic surfactant. 2018; <https://doi.org/10.5281/zenodo.1288297>.
- (96) Dvinskikh, S. V.; Zimmermann, H.; Maliniak, A.; Sandstrom, D. Measurements of motionally averaged heteronuclear dipolar couplings in MAS NMR using R-type recoupling. *J. Magn. Reson.* **2004**, *168*, 194–201.

- (97) Browning, J. L.; Seelig, J. Bilayers of phosphatidylserine: a deuterium and phosphorus nuclear magnetic resonance study. *Biochemistry* **1980**, *19*, 1262–1270.
- (98) Melcr, J. POPC lipid membrane, 303K, Charmm36 force field, simulation files and 200 ns trajectory for Gromacs MD simulation engine v5.1.2. 2016; <https://doi.org/10.5281/zenodo.153944>.
- (99) Favela-Rosales, F. MD simulation trajectory of a lipid bilayer: Pure POPC in water. SLIPIDS, Gromacs 4.6.3. 2016. 2016; <https://doi.org/10.5281/zenodo.166034>.
- (100) Hauser, H.; Shipley, G. G. Interactions of monovalent cations with phosphatidylserine bilayer membranes. *Biochemistry* **1983**, *22*, 2171–2178.
- (101) Hauser, H.; Shipley, G. Comparative structural aspects of cation binding to phosphatidylserine bilayers. *Biochimica et Biophysica Acta (BBA) - Biomembranes* **1985**, *813*, 343 – 346.
- (102) Mattai, J.; Hauser, H.; Demel, R. A.; Shipley, G. G. Interactions of metal ions with phosphatidylserine bilayer membranes: effect of hydrocarbon chain unsaturation. *Biochemistry* **1989**, *28*, 2322–2330.
- (103) Cevc, G. Membrane electrostatics. *Biochim. Biophys. Acta - Rev. Biomemb.* **1990**, *1031*, 311 – 382.
- (104) Kim, S.; Patel, D.; Park, S.; Slusky, J.; Klauda, J.; Widmalm, G.; Im, W. Bilayer Properties of Lipid A from Various Gram-Negative Bacteria. *Biophysical Journal* **2016**, *111*, 1750 – 1760.
- (105) Nencini, R. Simulation data for CHARMM36 POPC bilayer, 100 lipids/leaflet, 310K, GROMACS 5.1.4. 2018; <https://doi.org/10.5281/zenodo.1198158>.
- (106) Nencini, R. Simulation data for CHARMM36 POPC bilayer, 100 lipids/leaflet, 450

mM CaCl₂ ("NB-Fix" used), 310K, GROMACS 5.1.4. 2018; <https://doi.org/10.5281/zenodo.1198171>.

- (107) Javanainen, M. POPC @ 310K, 450 mM of CaCl₂. Charmm36 with default Charmm ions. 2016; <http://dx.doi.org/10.5281/zenodo.51185>.